The *U2AF1*^{S34F} mutation induces lineage-specific splicing alterations in myelodysplastic syndromes

Bon Ham Yip[1], Violetta Steeples[1], Emmanouela Repapi[2], Richard N. Armstrong[1], Miriam Llorian[3], Swagata Roy[1], Jacqueline Shaw[1], Hamid Dolatshad[1], Stephen Taylor[2], Amit Verma[4], Matthias Bartenstein[4], Paresh Vyas[5], Nicholas C. P. Cross[6], Luca Malcovati[7], Mario Cazzola[7], Eva Hellström-Lindberg[8], Seishi Ogawa[9], Christopher W. J. Smith[3], Andrea Pellagatti[1*], Jacqueline Boultwood[1*]

[1] Bloodwise Molecular Haematology Unit, Nuffield Division of Clinical Laboratory Sciences, Radcliffe Department of Medicine, University of Oxford, and BRC Blood Theme, NIHR Oxford Biomedical Centre, Oxford University Hospital, Oxford, UK
[2] The Computational Biology Research Group, Weatherall Institute of Molecular Medicine, University of Oxford, Oxford, UK
[3] Department of Biochemistry, Downing Site, University of Cambridge, Cambridge, UK
[4] Albert Einstein College of Medicine, Bronx, New York
[5] Medical Research Council, Molecular Hematology Unit, Weatherall Institute of Molecular Medicine, University of Oxford, and Department of Hematology, Oxford University Hospital National Health Service Trust, Oxford, UK
[6] Faculty of Medicine, University of Southampton, Southampton, and National Genetics Reference Laboratory (Wessex), Salisbury, UK
[7] Fondazione IRCCS Policlinico San Matteo and University of Pavia, Pavia, Italy
[8] Center for Hematology and Regenerative Medicine, Karolinska University Hospital Huddinge, Stockholm, Sweden
[9] Department of Pathology and Tumor Biology, Kyoto University, Kyoto, Japan

[*]A. Pellagatti and J. Boultwood contributed equally to this paper.

Corresponding author:
Professor Jacqueline Boultwood
Bloodwise Molecular Haematology Unit
Nuffield Division of Clinical Laboratory Sciences
Radcliffe Department of Medicine, University of Oxford
John Radcliffe Hospital
Oxford OX3 9DU
United Kingdom
Telephone: +44 1865 220480
Fax Number: +44 1865 221778
Email: jacqueline.boultwood@ndcls.ox.ac.uk

Conflict of interest
The authors have declared that no conflict of interest exists

Abstract

Mutations of the splicing factor *U2AF1* are frequent in the myeloid malignancy myelodysplastic syndromes (MDS) and in other cancers. Patients with MDS suffer from peripheral blood cytopenias, including anemia, and increasing bone marrow blasts. We investigated the impact of the common *U2AF1*^{S34F} mutation on cellular function and mRNA splicing in the main cell lineages affected in MDS. We demonstrated that *U2AF1*^{S34F} expression in human hematopoietic progenitors impairs erythroid differentiation, and skews granulomonocytic differentiation towards granulocytes. RNA-sequencing of erythroid and granulomonocytic colonies revealed that *U2AF1*^{S34F} induced a higher number of cassette exon splicing events in granulomonocytic than erythroid cells, and altered mRNA splicing of many transcripts (expressed in both cell types) in a lineage-specific manner. The introduction of isoform changes identified in the target genes *H2AFY* and *STRAP* into hematopoietic progenitors recapitulated phenotypes associated with *U2AF1*^{S34F} expression in erythroid and/or granulomonocytic cells, suggesting a causal link. Importantly, we provided evidence showing that isoform modulation of the *U2AF1*^{S34F} target genes *H2AFY* and *STRAP* rescues the erythroid differentiation defect in *U2AF1*^{S34F} MDS cells, raising the possibility of using splicing modulators therapeutically. These data have critical implications for understanding MDS phenotypic heterogeneity, and for the development of new targeted therapies.

Introduction

The myelodysplastic syndromes (MDS) are a heterogeneous group of clonal hematopoietic stem cell malignancies characterized by ineffective hematopoiesis resulting in peripheral blood cytopenias of the myeloid lineage, including anemia and neutropenia. MDS patients show increasing bone marrow myeloid blasts as the disease progresses and approximately 40% of MDS patients develop acute myeloid leukemia (AML). MDS is as common as de novo AML, with an incidence of 4/100,000/year (1-4). Patients with the more advanced MDS subtypes (refractory anemia with excess blasts 1 and 2), have a median overall survival of <2 years, highlighting the severity of these diseases (1, 2, 4). The recent finding that splicing factor genes are the most commonly mutated genes found in MDS (5, 6) revealed a new leukemogenic pathway involving spliceosomal dysfunction in this disorder. Over half of all MDS patients carry spliceosome gene mutations (6, 7), with *SF3B1*, *SRSF2*, *U2AF1* and *ZRSR2* being the most frequently mutated splicing factor genes (6). The common spliceosome mutations in MDS have differing prognostic impacts (8-10) and to some extent define distinct clinical phenotypes (5, 8, 11). While at present there is not extensive direct evidence that the alterations in pre-mRNA splicing caused by mutations in splicing factors are the main mechanism driving the disease in MDS, aberrant splicing of some key downstream target genes (e.g. *ABCB7* and *EZH2*) linked to splicing factor gene (*SF3B1* and *SRSF2*) mutations has been shown to be associated with certain MDS disease aspects/phenotypes (12, 13).

Pre-mRNA splicing involves the excision of intronic sequences from pre-mRNAs (14) and is performed by the spliceosome, a complex of five small nuclear ribonucleoproteins (snRNPs) and other supplementary proteins. U2AF1 (U2AF35) is a U2 auxiliary factor that forms a

heterodimer with U2AF2 (U2AF65) for the recognition of the 3' splice site and subsequent recruitment of U2 snRNP during pre-mRNA splicing (15, 16). Mutations in *U2AF1* have been found in approximately 11% of patients with MDS (6, 17), making *U2AF1* one of the most commonly mutated genes in this disease. Mutations in *U2AF1* also occur in the closely related condition AML at a frequency of approximately 4% (18) and in lung adenocarcinoma and other cancers (18, 19). *U2AF1* mutations are associated with worse overall survival in MDS patients and higher risk of transformation to AML (11, 20, 21). *U2AF1* mutations almost exclusively occur in two highly conserved amino acid positions, S34 and Q157, within the two zinc finger domains of the protein (6). There is clear evidence in yeast showing that the zinc finger domains in U2AF1 recognize RNA (6). The high % of sequence identity in the zinc finger domains between yeast and human (6) suggests that the zinc finger domains in human U2AF1 are also RNA binding (22). The presence of missense mutational hotspots and the absence of nonsense/frameshift mutations suggest that *U2AF1* mutations are gain of function or change of function/neomorphic mutations (6).

Abnormal RNA splicing, with cassette exon splicing being the most frequent type of event, has been reported in *U2AF1* mutant MDS and AML patient bone marrow samples (18, 23, 24). Several studies demonstrated that differentially spliced exons exhibited different consensus nucleotides at the -3 and +1 positions flanking the AG dinucleotide of the 3' splice site (18, 23-25). Thymidine (uridine) was observed less frequently than cytosine at the -3 position of the 3' splice site in the U2AF1 S34F mutant compared to U2AF1 wild-type samples (18, 23, 25).

Recently, Shirai et al. generated a doxycycline-inducible transgenic mouse model of *U2AF1* S34F mutation displaying some phenotypes that are closely associated with MDS (26). This

transgenic murine model sheds light on the role of this mutation in altering hematopoesis and pre-mRNA splicing in the mouse (26). The investigation of the lineage-specific effect of *U2AF1* S34F mutation on human hematopoiesis could provide new insights into the molecular pathogenesis of U2AF1 mutant MDS and illuminate how this mutation impacts the MDS phenotype.

Here we demonstrate that the *U2AF1* S34F mutation exhibits lineage specificity in altering pre-mRNA splicing of downstream target genes, resulting in different phenotypes in the different myeloid lineages that are involved in MDS.

Results

Expression of *U2AF1*^{S34F} in hematopoietic progenitors

To investigate the impact of the *U2AF1* S34F mutation on erythroid and granulomonocytic differentiation, we first overexpressed U2AF1 S34F mutant (*U2AF1*^{S34F}) and U2AF1 wild-type (*U2AF1*^{WT}) in primary human bone marrow CD34^{+} progenitor cells by retroviral transduction. Transduced progenitor cells were then cultured under erythroid or granulomonocytic conditions for differentiation into erythroid and granulomonocytic cells respectively (Supplemental Figure 1A). The gene expression level of *U2AF1*^{S34F} and *U2AF1*^{WT} compared to empty vector (EV) control was confirmed by real-time quantitative PCR in transduced cells harvested on day 11 (Supplemental Figure 1B). The expression of the *U2AF1*^{S34F} in transduced cells was confirmed by Sanger sequencing (Supplemental Figure 1C). Expression of U2AF1^{S34F} and U2AF1^{WT} protein in transduced cells harvested on day 11 was demonstrated by anti-FLAG and anti-U2AF1 antibodies (Figure 1A and Figure 2A). Overexpression of exogenous U2AF1^{S34F} and U2AF1^{WT} protein driven by retroviral vectors (anti-FLAG antibody) resulted in a modest increase (approximately 1.5-2.0 fold increase, i.e. not a large excess compared to the levels observed in the EV control) in the total U2AF1 protein levels (anti-U2AF1 antibody) in *U2AF1*^{S34F} and *U2AF1*^{WT} transduced cells throughout erythroid and granulomonocytic differentiation (Supplemental Figure 1D).

U2AF1^{S34F} impairs erythroid differentiation

To investigate the effect of the *U2AF1*^{S34F} on erythroid differentiation, transduced hematopoietic progenitors were cultured using a method developed to study the generation of

erythroblasts (27) and erythroblasts were harvested on day 11 and day 14 of culture for the measurement of the erythroid cell surface markers CD71 and CD235a by flow cytometry (Figure 1, B to E). A significant increase in the $CD71^{-}CD235a^{-}$ non-erythroid cell population (Figure 1B) and a significant decrease in $CD71^{+}CD235a^{+}$ intermediate erythroid cell population (Figure 1C) was observed in *U2AF1*^{S34F} erythroblasts on day 11 compared to the *U2AF1*^{WT} and EV controls. A decrease in late $CD71^{-}CD235a^{+}$ erythroid cell population was observed in *U2AF1*^{S34F} erythroblasts on day 14 compared to the *U2AF1*^{WT} and EV controls (Figure 1, D and E). The examination of erythroblasts on day 14 revealed that *U2AF1*^{S34F} erythroblasts exhibited defective hemoglobinization compared to the *U2AF1*^{WT} and EV controls (Figure 1F). To further characterize the effect of *U2AF1*^{S34F} on erythroid differentiation, we performed colony forming cell assays and found that *U2AF1*^{S34F} transduced progenitors produced a significantly lower number of burst-forming unit-erythroid (BFU-E) colonies compared to the *U2AF1*^{WT} and EV controls after 14 days in culture (Figure 1G). Morphological examination of BFU-E colonies revealed that *U2AF1*^{S34F} inhibited colony growth, resulting in smaller colonies, and impaired hemoglobinization (Figure 1H). Transduced erythroblasts underwent Geneticin selection on day 3 following retroviral transduction. They were harvested on day 8 for cell growth assays until day 14 in culture (Figure 1I). *U2AF1*^{S34F} erythroblasts exhibited impaired cell growth compared to the *U2AF1*^{WT} and EV controls (Figure 1I). No change in cell cycle pattern was observed among samples (Supplemental Figure 1E), but a significant increase in apoptosis was observed in *U2AF1*^{S34F} erythroblasts harvested on day 11 compared to the *U2AF1*^{WT} and EV controls (Figure 1J). These results indicate that *U2AF1*^{S34F} impaired cell growth and increased apoptosis in erythroblasts, and led to impaired differentiation.

_U2AF1_^{S34F} skews granulomonocytic differentiation towards granulocytes

To investigate the effects of *U2AF1*^{S34F} on the granulomonocytic differentiation, transduced hematopoietic progenitors were cultured under granulomonocytic differentiating conditions (28) and granulomonocytic cells were harvested on day 11 and day 14 of culture for measurement of the myeloid cell surface markers CD11b, CD14 and CD15 by flow cytometry. CD11b is a myeloid cell surface marker expressed on granulocytes, monocytes and macrophages (29). CD14 and CD15 are expressed predominantly on monocytes and granulocytes respectively, and were used as lineage discriminators between monocytic and granulocytic cell populations (30). Based on the signal intensity of forward scatter (as a measure of cell size), *U2AF1*^{S34F} granulomonocytic cells were larger than the *U2AF1*^{WT} and EV controls (Figure 2B and Supplemental Figure 1F). A significant decrease in the CD11b^{+} cell population was observed in *U2AF1*^{S34F} granulomonocytic cells compared to the *U2AF1*^{WT} and EV controls on day 11 and day 14 (Figure 2C). However, no difference in CD14^{+} and CD15^{+} cell populations was observed among samples at these two time points (data not shown). *U2AF1*^{S34F} granulomonocytic cells exhibited impaired cell growth compared to the *U2AF1*^{WT} and EV controls (Figure 2D). No difference in apoptosis was observed in *U2AF1*^{S34F} granulomonocytic cells (Supplemental Figure 1G), however *U2AF1*^{S34F} triggered a G2/M cell cycle arrest in granulomonocytic cells compared to the *U2AF1*^{WT} and EV controls (Figure 2E). These data show impaired growth and differentiation in *U2AF1*^{S34F} granulomonocytic cells.

Granulomonocytic differentiation was also evaluated on day 20 of culture, and a significant decrease in the CD11b^{+} cell population was observed in *U2AF1*^{S34F} granulomonocytic cells compared to the *U2AF1*^{WT} and EV controls (Figure 2F). Moreover, a significant decrease in the CD14^{+} monocytic cell population and a concomitant significant increase in the CD15^{+}

granulocyic cell population was observed in *U2AF1*^{S34F} granulomonocytic cells compared to the *U2AF1*^{WT} and EV controls, indicating a skewing effect of *U2AF1*^{S34F} on granulomonocytic differentiation (Figure 2, G to I). To confirm this phenotype, granulomonocytic cells were stained with May-Grünwald and Giemsa for morphological examination (Figure 2, J and K). Consistent with flow cytometry data (Figure 2, G to I), an expansion of the granulocyte population, specifically eosinophils, was observed in *U2AF1*^{S34F} granulomonocytic cells compared to the *U2AF1*^{WT} and EV controls (Figure 2, J and K). Furthermore, *U2AF1*^{S34F} transduced progenitors produced a significantly lower number of CFU-M colonies and a significantly higher number of CFU-G colonies in myeloid colony forming cell assays (Figure 2L). Our results indicate that *U2AF1*^{S34F} perturbs granulomonocytic cells by skewing their differentiation from monocytes towards granulocytes.

U2AF1^{S34F} differentially alters splicing in erythroid and granulomonocytic colonies

In order to investigate the effects of the presence of the *U2AF1*^{S34F} on pre-mRNA splicing in cells committed towards the myeloid or erythroid lineage, we performed RNA sequencing on individual erythroid and granulomonocytic colonies formed in colony forming cell assays by bone marrow CD34^{+} cells transduced with *U2AF1*^{S34F}, *U2AF1*^{WT} or EV. The *U2AF1*^{S34F} variant allele frequency was >80% in erythroid and granulomonocytic colonies expressing the U2AF1 S34F mutation, as measured by pyrosequencing (Figure 3A). Replicate MATS (rMATS), a computational tool designed for the detection of differential alternative splicing from replicate RNA-seq data (31), was used for RNA-seq data analysis. A total of 506 splicing events (347 genes) and 439 splicing events (300 genes) were identified in *U2AF1*^{S34F} erythroid colonies compared to the *U2AF1*^{WT} and EV control respectively (Supplementary

Data 1). A total of 643 splicing events (447 genes) and 676 splicing events (474 genes) were identified in *U2AF1*^{S34F} granulomonocytic colonies compared to the *U2AF1*^{WT} and EV control respectively (Supplementary Data 1). Alteration in cassette exon splicing (i.e. exons which are either included or spliced out, showing increased or decreased inclusion levels respectively), was the most common type of aberrant splicing event induced by *U2AF1*^{S34F} in both erythroid and granulomonocytic colonies (Figure 3, B and C). A significantly higher number of regulated cassette exon events was observed in granulomonocytic *U2AF1*^{S34F} colonies compared to erythroid *U2AF1*^{S34F} colonies in both comparisons with the *U2AF1*^{WT} and EV controls (Figure 3, B and C). This increase in the numbers of cassette exon events accounts for the higher numbers of total aberrant splicing events associated with granulomonocytic *U2AF1*^{S34F} colonies compared to erythroid *U2AF1*^{S34F} colonies (Figure 3, B and C).

We investigated the properties of misregulated cassette exons and cassette exons that were unaffected by *U2AF1*^{S34F} compared to *U2AF1*^{WT} (Figure 3D and Supplemental Figure 2). Cassette exons that were more included, or that were unregulated showed the normal preference for CAG 3' splice sites. In contrast, exons that were more skipped in response to *U2AF1*^{S34F} showed a strong enrichment for TAG 3' splice sites (Figure 3D, position 33 on sequence logos), as observed previously (18, 23, 24, 26). These exons also had significantly weaker 5' splice sites compared to *U2AF1*^{S34F} unregulated exons (Supplemental Figure 2). Their 3' splice sites were also weaker than unregulated exons (erythroid only), while their branch point strengths did not differ significantly. While we could readily detect differences between exons that were more included or skipped in response to *U2AF1*^{S34F}, we observed no differences between the properties of exons regulated in erythroid or granolumonocytic cells. However, we did observe that the majority of regulated cassette exons (*U2AF1*^{S34F} vs

253 *U2AF1*^{WT}) were more skipped in erythroid cells (60% more skipped), while in
254 granulomonocytic cells only 45% were more skipped (Figure 3E).
255
256 The number of genes showing significant aberrant splicing events in both comparisons of
257 *U2AF1*^{S34F} with EV and *U2AF1*^{S34F} with *U2AF1*^{WT} were 112 in erythroid colonies and 217 in
258 granulomonocytic colonies (Figure 3F and Supplementary Data 2). A total of 92 genes
259 showed aberrant splicing events in erythroid colonies only, and 197 genes in
260 granulomonocytic colonies only (Figure 3F and Supplementary Data 2). The large majority
261 (≥95%) of these genes aberrantly spliced in either erythroid or granulomonocytic lineage only
262 were also expressed in the other lineage (Supplemental Figure 3 A). Twenty genes were
263 common in the lists of aberrantly spliced genes in erythroid and granulomonocytic
264 *U2AF1*^{S34F} colonies (Figure 3F and Supplementary Data 2). For the genes that were
265 differentially spliced in the erythroid lineage, we found that the distribution of their
266 expression levels (log2rpkm) was comparable in the erythroid and granulomonocytic lineage.
267 Similarly, for the genes that were differentially spliced in the granulomonocytic lineage, we
268 found that the distribution of their expression levels (log2rpkm) was comparable in the
269 erythroid and granulomonocytic lineage (Supplemental Figure 3 B). The limited overlap of
270 aberrantly spliced genes between erythroid and granulomonocytic colonies suggests that the
271 splicing of different set of genes was altered in erythroid and granulomonocytic lineages. We
272 performed gene ontology analysis on the lists of significant genes showing aberrant splicing
273 events identified by the rMATS pipeline using GOseq. The significant main ontology themes
274 for the comparison of erythroid *U2AF1*^{S34F} colonies to EV and/or *U2AF1*^{WT} are related to
275 heme processing and mRNA processing (Supplementary Data 3 and 4). Taken together, these
276 data indicate that *U2AF1*^{S34F} alters target genes in a lineage-specific manner, driving different
277 phenotypes in different myeloid lineages.

To identify common aberrantly spliced genes associated with *U2AF1* mutations, we have performed a comparison of our RNA-seq data on *U2AF1*^{S34F} erythroid and granulomonocytic cells with RNA-seq data from other studies, including CMPs from a U2AF1 S34F transgenic mouse (26) and AML patient samples with *U2AF1* S34 mutations (23) (Figure 3, G and H; Supplementary Data 5 and 6). Approximately 10% and 30% of the aberrantly spliced genes in our RNA-seq dataset on erythroid and granulomonocytic colonies were also present in the studies of mouse CMPs and AML patient samples respectively (Figure 3, G and H; Supplementary Data 5 and 6). The genes that are shared across datasets represent important targets of U2AF1^{S34F}.

Moreover, we performed RNA sequencing on bone marrow CD34^{+} cells of two MDS cases with *U2AF1*^{S34F} mutation, four MDS cases without known mutations in splicing factor genes and five healthy controls. We have compared the lists of aberrantly spliced genes identified by rMATS in the comparison of *U2AF1*^{S34F} MDS cases versus MDS cases without splicing factor gene mutations and versus healthy controls, with the lists of aberrantly spliced genes that we identified in *U2AF1*^{S34F} transduced erythroid and granulomonocytic colonies. We found that approximately 40% of the aberrantly spliced genes identified in *U2AF1*^{S34F} transduced erythroid and granulomonocytic colonies respectively were also present in the lists of aberrantly spliced genes in the comparisons of *U2AF1*^{S34F} MDS cases versus MDS cases without splicing factor gene mutations and versus healthy controls (Figure 3, I and J; Supplementary Data 1, 7 and 8).

Differences in the number of differentially spliced target genes identified in *U2AF1*^{S34F} transduced erythroid and granulomonocytic colonies in our study and the number of

differentially spliced target genes identified in the other datasets mentioned above are likely due to differences in the RNAseq analysis pipeline and/or filtering cut-off values, as well as the cell type analyzed.

Confirmation of splicing alterations in *U2AF1*^{S34F} erythroid and granulomonocytic cells

Several aberrantly spliced genes in *U2AF1*^{S34F} erythroid and granulomonocytic colonies were selected for confirmation of the splicing abnormality identified using rMATS. The genes were chosen on the basis of the following criteria: abnormal splicing identified in our study and also in the *U2AF1*^{S34F} transgenic mouse CMPs and/or TCGA AML patient samples with *U2AF1* S34 mutation (18, 23, 26), known biological function (particularly regarding hematopoiesis) and previously described involvement in tumorigenesis. We selected the *H2AFY*, *STRAP*, *SMARCA5*, *ITGB3BP* and *ATR* genes for confirmation of the mutant U2AF1-induced splice isoform changes identified by RNA-seq in these five genes using real-time quantitative PCR, and RT-PCR and gel electrophoresis.

A mutually exclusive exon splicing alteration in *H2AFY* was identified in both *U2AF1*^{S34F} erythroid and granulomonocytic colonies (Figure 4, A to C). Decreased usage of exon 6b (which is mutually exclusive to exon 6a) in the *H2AFY* gene, was observed in both *U2AF1*^{S34F} erythroid and granulomonocytic colonies compared to the corresponding *U2AF1*^{WT} and EV controls (Figure 4, B and C). Aberrant splicing of *STRAP* and *SMARCA5* was observed in cells of the erythroid lineage only (Figure 4, A, D and E; Supplemental Figure 4 A and C), while splicing alteration of *ITGB3BP* and *ATR* were found only in granulomonocytic cells (Supplemental Figure 4 A, B and D). Increased skipping of exon 2 of *STRAP* (Figure 4, D and E) and skipping of exon 14 of *SMARCA5* (Supplemental Figure 4C)

in *U2AF1*^{S34F} cells compared to the *U2AF1*^{WT} and EV controls occurred preferentially in erythroid cells. In contrast, inclusion of exon 2 of *ITGB3BP* and inclusion of exon 47 of *ATR* were associated with *U2AF1*^{S34F} granulomonocytic cells (Supplemental Figure 4, B and D). To confirm these splicing alterations, we performed isoform-specific real-time quantitative PCR, and RT-PCR and gel electrophoresis, to measure the isoform changes associated with U2AF1^{S34F} in transduced erythroid and granulomonocytic cells, and all splicing alterations were concordant with the RNA-Seq data (Figure 4, B and D and Supplemental Figure 4, B to D). Moreover, the full-length isoforms and the aberrant splice junctions of selected genes (*H2AFY* and *STRAP*) were all confirmed by Sanger sequencing (Supplemental Figures 5 and 6). Our data show that U2AF1^{S34F} differentially alters splicing of target genes in a lineage-specifc manner in erythroid and granulomonocytic lineages, supporting the hypothesis that the same splicing factor gene mutation can drive aberrant splicing of distinct genes in different cell populations.

Park et al recently reported selection of a distal cleavage and polyadenylation (CP) site in the autophagy-related factor 7 (Atg7) pre-mRNA in association with the presence of the *U2AF1*^{S34F} mutation (32). This results in a decrease in ATG7 levels leading to defective autophagy, making cells more prone to secondary mutations (32). We performed real-time quantitative PCR to evaluate selection of the distal CP site of ATG7 (32) in *U2AF1*^{S34F} erythroid and granulomonocytic colonies in our study. We did not observe increased usage of the distal CP site of ATG7 in *U2AF1*^{S34F} granulomonocytic cells (distal/proximal CP site usage ratio 1.03 and 0.98 in *U2AF1*^{S34F} and *U2AF1*^{WT} respectively compared to the EV), however this represents a different cell population from that studied by Park et al (32). The expression of ATG7 was too low for assessment in *U2AF1*^{S34F} erythroid cells.

Functional effects of splicing aberrations associated with the *U2AF1*^{S34F}

We performed functional studies to determine the impact of the splicing abnormalities identified in *H2AFY*, *STRAP* and *ITGB3BP* on human erythroid and/or granulomonocytic cell growth and differentiation.

Usage of the mutually exclusive exons 6a and 6b in the *H2AFY* gene gives rise to the two transcript isoforms 1.2 and 1.1 respectively. Our RNA sequencing data showed that *U2AF1*^{S34F} was associated with altered pre-mRNA splicing of *H2AFY*, with decreased usage of exon 6b resulting in a decrease in the expression levels of the isoform 1.1 of this gene in both erythoid and granulomonocytic colonies. To investigate the effects of reduced expression of the *H2AFY* isoform 1.1 on human hematopoiesis, we designed shRNAs to specifically knock down the *H2AFY* isoform 1.1 (Figure 5, A and G) without affecting the expression of the *H2AFY* isoform 1.2 (Figure 5, B and H) in bone marrow $CD34^+$ progenitor cells. Transduced progenitor cells were cultured under erythroid and granulomonocytic conditions as previously described (27, 28). Erythroblasts with *H2AFY* isoform 1.1 knockdown showed increased apoptosis (Supplemental Figure 7A) and G1 cell cycle arrest (Supplemental Figure 7B). Similarly to erythroblasts expressing *U2AF1*^{S34F}, erythroid cells with *H2AFY* isoform 1.1 knockdown exhibited defective hemoglobinization on day 14 of culture compared to the scramble shRNA control (Figure 5C). Furthermore, erythroblasts with *H2AFY* isoform 1.1 knockdown showed a significant decrease in the $CD71^+CD235a^+$ intermediate erythroid cell population on day 11 (Figure 5D), followed by a decrease in the $CD71^-CD235a^+$ late erythroid cell population on day 14 compared to the scramble control (Figure 5E). Transduced progenitors with *H2AFY* isoform 1.1 knockdown also produced a significantly lower number of BFU-E colonies compared to the scramble control (Figure 5F).

Granulomonocytic cells with *H2AFY* isoform 1.1 knockdown (Figure 5, G and H) showed a significant increase in the $CD14^{+}CD15^{+}$ cell population compared to the scramble control (Figure 5I), and *H2AFY* isoform 1.1 knockdown exerted a skewing effect on granulomonocytic differentiation towards granulocytes (Figure 5J). Morphological examination confirmed the expansion of granulocyte eosinophils in granulomonocytic cultures with *H2AFY* isoform 1.1 knockdown compared to the scramble control on day 20 of culture (Figure 5K). Granulomonocytic cells with knockdown of the *H2AFY* isoform 1.1 showed increased apoptosis (Supplemental Figure 7C), and no significant change in cell cycle (Supplemental Figure 7D). Our data indicate that *H2AFY* plays an important role in human hematopoiesis and that decreased expression of the isoform 1.1 expression associated with aberrant splicing of *H2AFY* in the presence of $U2AF1^{S34F}$ impairs both erythroid and granulomonocytic differentiation.

In this study, we showed that $U2AF1^{S34F}$ induced skipping of exon 2 of the *STRAP* gene preferentially in erythroid colonies compared to granulomonocytic colonies (Figure 4, D and E). This splicing alteration gives rise to a premature stop codon, which is expected to lead to degradation of the mRNA transcripts by nonsense-mediated decay. Indeed, we found decreased expression of the *STRAP* mRNA in $U2AF1^{S34F}$ erythroid cells by qRT-PCR (Supplemental Figure 7E). In contrast, downregulation of *STRAP* mRNA was not observed in $U2AF1^{S34F}$ granulomonocytic cells (Supplemental Figure 7F). To investigate the effects of this lineage-specific splicing alteration on hematopoiesis, shRNAs were used to knock down *STRAP* expression in bone marrow $CD34^{+}$ progenitor cells differentiated towards the erythroid lineage (Figure 6A). One shRNA (sh66) resulted in ~50% knockdown (Figure 6A), a similar level to that observed in $U2AF1^{S34F}$ erythroid cells (Supplemental Figure 7E). Erythroblasts with *STRAP* knockdown showed G1 cell cycle arrest compared to the scramble

control (Figure 6B). Similar to *U2AF1*^{S34F} erythroblasts, erythroblasts with *STRAP* knockdown exhibited defective hemoglobinization on day 14 (Figure 6C) and a significant decrease in CD71^{-}CD235a^{+} late erythroid cell population on day 14 of culture compared to the scramble control (Figure 6D). Transduced progenitors with *STRAP* knockdown also produced a significantly lower number of BFU-E colonies compared to the scramble control (Figure 6E). These results support a critical role for *STRAP* in human erythroid differentiation.

Inclusion of exon 2 of *ITGB3BP* was associated with the presence of *U2AF1*^{S34F} in granulomonocytic cells only in our study. To investigate the effect of this splicing alteration on hematopoiesis, the isoform of *ITGB3BP* including exon 2 was overexpressed in bone marrow CD34^{+} progenitor cells differentiated towards the granulomonocytic lineage (Figure 6F). However, granulomonocytic cells with *ITGB3BP* overexpression showed no significant difference in cell cycle pattern (Figure 6G) and apoptosis (Supplemental Figure 7G). Only a small reduction in the CD14^{+} monocytic cell population (Figure 6, H and J) and no difference in CD15^{+} granulocytic cell population (Figure 6, I and J) were observed in cells with *ITGB3BP* overexpression compared to the EV control. Morphological examination confirmed that no skewing in granulomonocytic differentiation occurred in cells with *ITGB3BP* overexpression (Figure 6K). These results indicate that overexpression of the isoform of *ITGB3BP* including exon 2, whilst associated with the presence of *U2AF1*^{S34F} in granulomonocytic cells, does not significantly impact human granulomonocytic differentiation.

Overexpression of U2AF1 wild-type in U2AF1 S34F mutant MDS hematopoietic progenitors

To investigate whether overexpression of U2AF1^{WT} rescues aberrant hematopoiesis associated with U2AF1^{S34F} in MDS, we overexpressed U2AF1^{WT} in *U2AF1*^{S34F} MDS hematopoietic progenitors by retroviral transduction. Overexpression of U2AF1^{WT} in transduced *U2AF1*^{S34F} MDS erythroid and granulomonocytic cells was confirmed on day 11 by Western blotting (Supplemental Figure 8A). However, no significant improvement in erythroid and granulomonocytic differentiation was observed in transduced *U2AF1*^{S34F} MDS cells with U2AF1^{WT} overexpression compared to the EV control (Supplemental Figure 8, B to D). Importantly, we found that overexpression of U2AF1^{WT} did not correct the aberrant splicing activity of *H2AFY* and *STRAP* in *U2AF1*^{S34F} MDS cells (Supplemental Figure 8, E to G), consistent with the gain-of-function/neomorphic role of *U2AF1*^{S34F}.

Overexpression of *H2AFY* isoform 1.1 and *STRAP* long isoform rescues erythroid differentiation defects in *U2AF1*^{S34F} MDS cells

In order to determine whether modulation of *H2AFY* and *STRAP* isoform ratios can rescue the aberrant hematopoiesis associated with U2AF1^{S34F}, we performed rescue experiments in which the *H2AFY* isoform 1.1 or *STRAP* long isoform were overexpressed in *U2AF1*^{S34F} MDS hematopoietic progenitors.

Firstly, we evaluated whether the aberrant splicing of *H2AFY* and *STRAP* occurs in the erythroid and granulomonocytic cells differentiated from *U2AF1*^{S34F} MDS hematopoietic progenitors. We differentiated *U2AF1*^{S34F} MDS CD34^{+} hematopoietic progenitor cells into erythroid and granulomonocytic cells as previously described (27, 28). Consistent with our RNA sequencing results of *U2AF1*^{S34F} transduced erythroid and granulomonocytic colonies (Figure 4), *U2AF1*^{S34F} MDS erythroid and granulomonocytic cells harvested on day 7 showed

a significant reduction in *H2AFY* isoform 1.1 compared to healthy controls (Figure 7A). *U2AF1*^{S34F} MDS erythroid cells harvested on day 7 also demonstrated a significant increase in the *STRAP* short isoform compared to healthy controls (Figure 7B). Aberrant splicing of *STRAP* was not observed in *U2AF1*^{S34F} MDS granulomonocytic cells harvested on day 7, further confirming our results of lineage-specific effect of *U2AF1* S34F mutation on this target gene (Figure 7B). Moreover, *U2AF1*^{S34F} MDS hematopoietic progenitors showed impaired erythroid differentiation on day 14 (Figure 7C) and skewed granulomonocytic differentiation towards granulocytes on day 20 (Figure 7, D and E) compared to healthy control cells.

Next, we overexpressed the *H2AFY* isoform 1.1 or *STRAP* long isoform in *U2AF1*^{S34F} MDS hematopoietic progenitors by lentiviral transduction. Overexpression of *H2AFY* isoform 1.1 in transduced *U2AF1*^{S34F} MDS erythroid and granulomonocytic cells was confirmed by RT-PCR compared to the EV control (Figure 7F). Overexpression of *STRAP* long isoform in transduced *U2AF1*^{S34F} MDS erythroblasts was also confirmed by RT-PCR compared to the EV control (Figure 7G). The percentage of $CD71^{-}CD235a^{+}$ erythroblasts on day 14 ranges 14.5%-17.2% in healthy controls (Figure 7C). Overexpression of the *H2AFY* isoform 1.1 resulted in an increase in late $CD71^{-}CD235a^{+}$ erythroblasts (to 5.7%-15.5%, i.e. 1.54-1.85 fold increase) on day 14 in the three *U2AF1*^{S34F} MDS cases with a trend toward significance compared to the EV control (Figure 7H). Overexpression of the *STRAP* long isoform resulted in a significant increase in late $CD71^{-}CD235a^{+}$ erythroblasts (to 6.5%-14.1%, i.e. 1.59-2.53 fold increase) on day 14 in the three *U2AF1*^{S34F} MDS cases compared to the EV control (Figure 7I). However, no change in monocytic and granulocytic cell differentiation was observed in transduced *U2AF1*^{S34F} MDS granulomonocytic cells with overexpression of *H2AFY* isoform 1.1 (Figure 7, J and K).

These results indicate that overexpression of *H2AFY* isoform 1.1 and *STRAP* long isoform rescues erythroid differentiation defects in *U2AF1*^{S34F} MDS cells.

Discussion

MDS patients suffer from refractory anemia and this is a defining feature of this disorder (1, 33). In our study we demonstrated that expression of the *U2AF1*^{S34F} in human hematopoietic progenitors results in impaired erythroid differentiation, due to poor hemoglobinization and reduced growth of erythroid progenitors. These in vitro results therefore show that the presence of the *U2AF1* mutation impairs human erythropoiesis and indicate that this mutation may play an important role in the development of anemia in MDS. Interestingly, it has been reported that *U2AF1* mutations are found in MDS patients associated with lower hemoglobin levels when compared to patients with wild-type *U2AF1* (34).

The MDS have a defective maturation programme of myeloid progenitors (1, 4). We showed that expression of the *U2AF1*^{S34F} in human hematopoietic progenitors results in the skewing of granulomonocytic differentiation towards granulocytes (specifically eosinophils). Similar phenotypes were also observed in the bone marrow compartment of an *U2AF1*^{S34F} transgenic mouse model (26): *U2AF1*^{S34F} mice showed a significant decrease in monocytes together with a significant increase in granulocyte neutrophils in the bone marrow compared to controls (26). Interestingly, eosinophilia has been reported in some patients with de novo MDS (35, 36). Our study demonstrates a link between *U2AF1*^{S34F} and skewed granulomonocytic differentiation in human hematopoiesis.

We found that expression of *U2AF1*^{S34F} has a suppressive effect on cell growth in transduced erythroid and granulomonocytic cells. Similarly, the introduction of the U2AF1 S34F mutation in cancer cell lines results in impaired cell growth (6), and this is also observed with

505 other splicing factor gene mutations (37). How splicing factor mutations confer a clonal
506 growth advantage in myeloid malignancies is not yet fully understood.
507
508 The phenotypic changes produced by the *U2AF1*^{S34F} likely reflect differences in the
509 downstream target genes/pathways affected in each lineage and in the type of aberrant
510 splicing events associated with the presence of *U2AF1*^{S34F}. In support of this, we identified
511 aberrant splicing events in many downstream target genes specific to *U2AF1*^{S34F} erythroid
512 and granulomonocytic colonies by RNA sequencing. Our RNA-seq data should be interpreted
513 with the caveats that the *U2AF1*^{S34F} expression level (at >80% VAF) in *U2AF1*^{S34F}
514 transduced cells is higher than the level expected in MDS patients with heterozygous *U2AF1*
515 mutations (i.e. 50% VAF) and that the *U2AF1*^{S34F} erythroid and granulomonocytic colonies
516 analyzed contain some heterogeneity in the stage of differentiation (but they are nevertheless
517 all fully committed towards either the myeloid or erythroid path). We suggest that the
518 aberrantly spliced target genes may play a role in the aberrant growth and differentiation of
519 cells of the erythroid and granulomonocytic lineages expressing this mutation.
520
521 Other studies have shown that aberrant cassette exon splicing is a common consequence of
522 *U2AF1* mutations (18, 23, 25), and we found that cassette exons were the most common type
523 of aberrant splicing event induced by *U2AF1*^{S34F} in both erythroid and granulomonocytic
524 colonies. Interestingly, a significantly higher number of misregulated cassette exon events
525 was observed in granulomonocytic *U2AF1*^{S34F} colonies compared to erythroid *U2AF1*^{S34F}
526 colonies in our study. Notably, the UAG 3' splice site signature of cassette exons that are
527 more skipped, is similar to the optimal RNA binding sequence for U2AF heterodimer (16),
528 strongly supporting the idea that mis-splicing of this group of exons is a direct consequence
529 of *U2AF1* mutation. The fact that these exons have significantly weaker 5' splice sites

suggests that their inclusion may be dependent upon optimal interaction of U2AF1 at their 3' splice sites, explaining their sensitivity to *U2AF1* mutation. Splicing of many exons is dependent not only upon the strength of their consensus splice site sequences, but also on auxiliary elements such as exon splicing enhancers (ESEs) (38). There are numerous classes of ESE, which bind different splicing activators often expressed with different cell-type specificity. Lineage and exon-specific skipping might therefore occur in the absence of the optimal U2AF1-3' splice site interaction (*U2AF1*^{S34F}) combined with cell-type specific lack of the ESE-binding activator protein. In contrast, the molecular basis of the increased inclusion of other cassette exons in response to *U2AF1*^{S34F} is unclear, although it has been observed previously that some exons are upregulated upon knockdown of U2AF1 (39).

In our study, we found that 20 genes were aberrantly spliced in cells of both erythroid and granulomonocytic lineages and thus represent common downstream targets of *U2AF1*^{S34F} that may play a role in the phenotypic changes observed in both lineages. *H2AFY* was one of these genes, showing a mutually exclusive exon splicing event in both lineages. *H2AFY* encodes the core histone macro-H2A1, which is involved in X chromosome inactivation (40) and is required for both transcriptional silencing and induction (41). Intriguingly, loss of X chromosome inactivation results in MDS-like phenotypes in mice (42). Alternative splicing in *H2AFY* has been shown to generate two functionally different isoforms (43). A role for macro histone variants in repressing gene expression during cell differentiation has been shown in embryonic and adult stem cells, and in pluripotent cells, where these variants are recruited to the regulatory regions of genes that retain or gain H3K27me3 during differentiation (44). *H2AFY* isoform 1.1 has been shown to be generally expressed in more differentiated cells (45). We found a reduction in the expression of isoform 1.1 of *H2AFY* associated with *U2AF1*^{S34F} in transduced erythroid cells. Critically, we then showed that

knockdown of the *H2AFY* isoform 1.1 in human erythroblasts results in impaired erythroid differentiation. Interestingly, isoform changes in *H2AFY* have been shown to play a role in normal erythroid differentiation. Pimentel et al. demonstrated that the relative expression of mutually exclusive exons is reversed almost completely between proerythroblasts (mostly expressing isoform 1.2) and orthochromatic erythroblasts (mostly expressing isoform 1.1), indicating that the alternative splicing switch from isoform 1.2 to isoform 1.1 of *H2AFY* occurs during normal late erythroid differentiation (46). Our data show that aberrant splicing of *H2AFY* associated with the presence of *U2AF1*^{S34F} leads to a reduction in the expression of isoform 1.1 of this gene. Here, the isoform 1.1 is the minor isoform (compared to isoform 1.2) and strikingly a small reduction in this isoform resulted in a marked impairment of erythropoiesis. We provide evidence that this imbalance of the two *H2AFY* isoforms prevents erythroblasts from undergoing terminal differentiation. We suggest that aberrant splicing of *H2AFY* leads to impaired erythropoiesis and may play a role in the anemia observed in MDS patients with *U2AF1* mutation.

We also found a reduction in the expression of isoform 1.1 of *H2AFY* associated with *U2AF1*^{S34F} in granulomonocytic cells. Knockdown of the *H2AFY* isoform 1.1 in granulomonocytic cells resulted in skewed differentiation towards the granulocyte population, specifically eosinophils, closely mirroring the effects of the *U2AF1*^{S34F} on granulomonocytic differentiation. Our functional data therefore indicate that changes in the abundance of *H2AFY* isoform 1.1 also plays a role in differentiation of granulomonocytic cells. Thus reduced expression of the *H2AFY* isoform 1.1 recapitulated the phenotypes associated with expression of *U2AF1*^{S34F} in erythroid and/or granulomonocytic cells, suggesting a causal link. Importantly, we showed that the aberrant splicing event in the

H2AFY gene that we identified in *U2AF1*^{S34F} erythroid and granulomonocytic colonies also occurs in purified bone marrow CD34^{+} cells of *U2AF1*^{S34F} MDS cases.

We have shown that *U2AF1*^{S34F} differentially alters mRNA splicing of many targets genes in a lineage-specific manner in erythroid and granulomonocytic colonies. For example, splicing alterations in *STRAP* and *SMARCA5* preferentially occur in the erythroid lineage while splicing alterations in *ITGB3BP* and *ATR* preferentially occur in the granulomonocytic lineage. STRAP is a serine/threonine kinase receptor associated protein which plays a role in the cellular distribution of the SMN complex, important in the assembly of small nuclear ribonucleoproteins (snRNPs) (47). Deregulated expression of *STRAP* is associated with other human cancers, including lung, colon, and breast cancers (48, 49).

In this study, we showed that *U2AF1*^{S34F} induced aberrant splicing of *STRAP* leading to downregulation of this gene in erythroid cells only, and that knockdown of *STRAP* in human erythroblasts results in impaired erythroid differentiation. These results support a critical role for *STRAP* in human erythroid differentiation and suggest that aberrant splicing of *STRAP* leads to impaired erythropoiesis in association with *U2AF1*^{S34F}. Interestingly, STRAP acts as a negative regulator of the TGF-beta signaling pathway through interaction with Smad7 (50), and TGF-β signaling exerts an inhibitory effect on erythroid cell growth during differentiation (51).

We have thus identified *H2AFY* and *STRAP* as key downstream target genes of *U2AF1*^{S34F} in human cells of the myeloid lineage, with aberrantly spliced *H2AFY* and *STRAP* both being critical effectors of impaired erythropoiesis and aberrantly spliced *H2AFY* also being a critical effector of aberrant granulomonocytic cell differentiation. While aberrant splicing of

these target genes leads to impaired differentiation of progenitor cells, in the stem cell compartment this might be predicted to result in a negative selection pressure on stem cells. We suggest that these splicing abnormalities play a role in the development of cytopenias that are hallmarks of MDS.

Importantly, we provide the first evidence showing that isoform modulation of the *U2AF1*^{S34F} target genes *H2AFY* and *STRAP* ameliorates the erythroid differentiation defect in *U2AF1*^{S34F} MDS cells. The overexpression of the *H2AFY* isoform 1.1 and the *STRAP* long isoform resulted in an improvement in erythroid differentiation, raising the possibility of using splicing modulators therapeutically. Approaches that involve the use of antisense/splice site switching oligonucleotides (ASO/SSO) alter the balance between mRNA isoforms with the aim to restore normal splicing or to preferentially express specific isoforms (52). ASO/SSO have shown efficacy in splicing modulation in in vivo mouse studies, and are being used in clinical trials for the treatment of spinal muscular atrophy and of Duchenne Muscular Dystrophy (53). The use of splicing modulators may have efficacy in the treatment of myeloid malignancies with *U2AF1* mutation.

No change in granulomonocytic differentiation was observed in transduced *U2AF1*^{S34F} MDS cells overexpressing *H2AFY* isoform 1.1, indicating that correction of a single isoform change of *H2AFY* may not be sufficient to fully rescue the defect in granulomonocytic differentiation in patient cells and that modulation of aberrant splicing of multiple target genes may be required.

We have also overexpressed *U2AF1*^{WT} in *U2AF1*^{S34F} MDS hematopoietic progenitors. However, no significant difference in erythroid or granulomonocytic differentiation was

observed between transduced *U2AF1*^{S34F} MDS cells with *U2AF1*^{WT} overexpression and EV controls. *U2AF1* mutations in myeloid malignancies are considered to be gain-of-function/neomorphic mutations. As *U2AF1*^{S34F} is still expressed in the MDS cells, it would continue to cause aberrant splicing of its target genes, and this may therefore explain why the overexpression of *U2AF1*^{WT} does not rescue the functional defects observed in *U2AF1*^{S34F} MDS cells. Alternatively, the U2AF1 mutation may exert its effect primarily early in MDS disease formation and the rescue is less effective at a later stage.

Our results demonstrate that *U2AF1*^{S34F} exhibits lineage specificity in altering pre-mRNA splicing of downstream target genes, resulting in different phenotypes in different myeloid lineages. These findings shed light on the events underlying the phenotypic heterogeneity in MDS. It will be important to determine whether other splicing factor genes commonly mutated in MDS, namely *SF3B1*, *SRSF2* and *ZRSR2*, also exhibit lineage specificity in altering the splicing of target genes to drive different phenotypes in different hematopoietic lineages.

The identification of key target genes of the common spliceosome mutations in cells of the erythroid and granulomonocytic lineage is crucial for understanding how the mutations contribute to MDS pathophysiology and for the design of new targeted therapeutic strategies. It is now recognized that splicing factor gene mutations are common in many cancers and our work has broad implications for the understanding of how these mutations result in cell type-specific phenotypes in other malignancies.

Methods

Cell culture

Bone marrow $CD34^+$ cells from healthy controls (Lonza) and *U2AF1*^{S34F} MDS patients were cultured for 14 and 20 days to generate erythroblasts and granulomonocytic cells respectively as previously described (27, 28). All cytokines were obtained from Miltenyi Biotec except erythropoietin was obtained from Roche. Medium was replenished every second day to maintain the same cell concentration.

Viral transduction

Retroviral pGCDNsam-IRES-eGFP plasmids containing *U2AF1*^{S34F} and *U2AF1*^{WT} cDNA were used following replacing the eGFP sequence by neomycin to impart G418 resistance (6). To obtain high-titer retrovirus stock, vector plasmids were co-transfected with Vesicular Stomatitis Virus Glycoprotein envelope and Gag/Pol plasmids using Lipofectamine 2000 (Life Technologies) into HEK293T cells as previous described (6). Spinoculation was performed in the presence of 8 μg/ml of polybrene (Sigma-Aldrich) at 800 × *g* at 32°C for 2 hours. After overnight incubation with retroviruses, selection of transduced cells was performed in medium containing Geneticin (Life Technologies) (0.75mg/ml and 1.0mg/ml for erythroid and granulomonocytic cells respectively).

Lentiviral constructs containing shRNAs targeting *H2AFY* isoform 1.1 were obtained by cloning oligos (shRNA sequences are described in Supplemental Table 1) into the pLKO.1-puro vector (Sigma-Aldrich). shRNAs targeting *STRAP* in the pLKO.1-puro vector (TRCN0000060465 and TRCN0000060466) were obtained from Sigma Mission. The lentiviral construct containing *ITGB3BP* isoform 1, *H2AFY* isoform 1.1 or *STRAP* long

isoform cDNA in the pReceiver-Lv156 vector was obtained from GeneCopoeia. The procedures of lentivirus production and transduction were the same as those used for retroviruses, except MISSION lentiviral packaging mix (Sigma-Aldrich) was used for transfection with vector plasmids into HEK293T cells. Selection of transduced cells was performed in medium containing 0.65μg/ml puromycin (Thermo Fisher Scientific).

Flow cytometry

To evaluate erythroid differentiation, cells were incubated for 30 minutes on ice with anti-CD36-PE (Clone 5-271; BioLegend), anti-CD71-FITC (Clone OKT9; eBioscience) and anti-CD235a-APC (Clone HIR2; BioLegend) antibodies before staining with 0.5μg/ml DAPI (Sigma Aldrich). To evaluate granulomonocytic differentiation, cells were first incubated for 30 minutes on ice with Fixable Viability Dye eFluor 780 (eBioscience). After washing with PBS, cells were then incubated on ice for 30 minutes with anti-CD11b-Brilliant Violet 421 (Clone ICRF44; BioLegend), anti-CD14-FITC (Clone RMO52; Beckman Coulter) and anti-CD15-APC (Clone W6D3; BioLegend) antibodies. To perform apoptosis assay, cells resuspended in Annexin V Binding Buffer (BioLegend) were stained with Annexin V-FITC antibody (BioLegend) for 20 minutes in the dark according to the manufacturer's instructions. 1μg/ml propidium iodide was added to the cells before analysis. To perform cell cycle analysis, cells were fixed with ice-cold absolute ethanol for 30 minutes before incubation with 40μg/ml propidium iodide and 10μg/ml RNase A for one hour at 37°C. Flow cytometry was performed on a BD LSRII (BD Bioscience) and the data were analysed using FlowJo software version 7.6.4.

Colony-forming cell assay

Colony-forming cell assays were performed using MethoCult H4434 and H4534 methylcellulose (StemCell Technologies) according to the manufacturer's instructions. Transduced cells (3,000 cells) were grown in methylcellulose containing 1.0mg/ml Geneticin. The number and morphology of the colonies were investigated after 14 days in culture.

RNA sequencing

Individual BFU-E colonies (n=3 each for *U2AF1*^{S34F}, *U2AF1*^{WT} and EV) and CFU-G/M colonies (n=3 each for *U2AF1*^{S34F}, *U2AF1*^{WT} and EV) were first harvested for RNA extraction using TRIzol according to manufacturer's instructions. RNA was extracted also from bone marrow CD34^{+} cells enriched from mononuclear cells of 6 MDS patients and 5 healthy controls using CD34 MicroBeads (Miltenyi Biotec, Bergisch Gladbach, Germany). Two MDS cases had *U2AF1*^{S34F} mutation, whereas four cases had no known mutations in splicing factor genes (*SF3B1, SRSF2, U2AF1* or *ZRSR2)* as determined by targeted next-generation sequencing data from a previous study (5). Linear acrylamide (Thermo Scientific) (20µg) was used as RNA co-precipitant. Total RNA was then DNase treated (Invitrogen), purified using XP beads (Beckman Coulter, High Wycombe, UK) and amplified (100 ng) for 12 cycles using SMART mRNA Amplification Kit (Clontech) according to manufacturer's instructions. Library preparation was performed using NEBNext DNA Library Prep Kit (NEB, Hitchin, UK) according to manufacturer's instruction. Illumina universal paired end adaptors were used. Custom indexes were designed in house to barcode sequences for multiplexing. Sequencing was performed using the Illumina HiSeq2500 platform (100bp read length, paired end) using reagent kit v3 (Illumina, San Diego, CA, USA).

Mapping, filtering and alternative splicing analysis

Following QC analysis with the fastQC package (http://www.bioinformatics.babraham.ac.uk/projects/fastqc), reads were aligned using STAR (54) against the human genome assembly (NCBI build37 (hg19) UCSC transcripts). QC was performed on the mapped files using RNA-SeQC (55) (Supplemental Table 2). Non-uniquely mapped reads and reads that were identified as PCR duplicates using Samtools (56) were discarded. Gene expression levels were quantified as read counts using the featureCounts function (57) from the Subread package (58) with default parameters and the RPKM values were generated using the edgeR package (59). The aligned reads were reconstructed into transcripts using Cufflinks (cuffmerge) (60) to produce a reference-guided assembly (with NCBI build37 (hg19) UCSC transcripts). Alternative 3′ and 5′ splice sites, skipped (cassette) exons, mutually exclusive exons, and retained introns were quantified using rMATS (31) with the assembly produced from Cufflinks. Splicing events were considered to be significantly different in *U2AF1*^{S34F} compared to the *U2AF1*^{WT} or EV control if they met the criteria of a false-discovery rate ≤0.05, a change in inclusion level ≥10% (23), and did not appear as significant events in the comparison between *U2AF1*^{WT} and EV (Supplementary Data 1). The alternative spliced events were then plotted using the sashimi plots of the MISO software (61). The results were visualised and filtered using the data visualisation tool Zegami (http://zegami.com/). Integrative Genomics Viewer (IGV) v2.3 (http://www.broadinstitute.org/igv/) was used for visualization of the sequence reads. The data discussed in this publication have been deposited in NCBI's Gene Expression Omnibus and are accessible through GEO Series accession number GSE94153.

Gene Ontology analysis

747 Gene Ontology analysis of the RNA-Seq data was performed using GOseq (62). A weighted
748 bias correction based on the number of exons in each gene from the NCBI build37 (hg19)
749 UCSC transcripts was applied.
750
751 **Isoform-specific real-time quantitative PCR and RT-PCR**
752 To determine the expression levels of specific isoforms of *H2AFY*, *STRAP*, *SMARCA5*,
753 *ITGB3BP* and *ATR*, primers were designed to span the region affected by aberrant splicing
754 induced by *U2AF1*^{S34F} (Supplemental Table 1). Expression levels of these isoforms were
755 measured by real-time quantitative PCR using LightCycler 480 SYBR Green I Master Mix
756 according to the manufacturer's instructions (Roche). The *GAPDH* gene was used to
757 normalize for differences in input cDNA using PrimePCR SYBR Green Assay: GAPDH,
758 Human (Bio-Rad). Each sample was run in triplicate and the expression ratios were
759 calculated using the $\Delta\Delta C_T$ method. To confirm the splicing events of *H2AFY* and *STRAP*,
760 RT-PCR was performed to amplify the region affected by aberrant splicing. Quantification of
761 different isoforms was achieved by agarose gel electrophoresis and ImageJ analysis.
762
763 **Analysis of cassette exon properties**
764 For analysis of cassette exon properties, we used "skipped exons" (SE) from the rMATS
765 output with FDR < 0.05, and IncLevelDifference < -0.10 ("more skipped") or > 0.10 ("more
766 included"). For each SE, we extracted sequences corresponding to its 3'ss and 5'ss as well as
767 sequences corresponding to the 5'ss of the upstream exon, and 3'ss of the downstream exon.
768 For the erythroid cells, *U2AF1*^{S34F} vs *U2AF1*^{WT} we obtained 71 exons more skipped, and 108
769 exons more included. For the granulomonocytic *U2AF1*^{S34F} vs *U2AF1*^{WT}, we obtained 190
770 more skipped exons and 157 more included exons. As control datasets, we have used SE
771 exons expressed in the erythroid and granulomonocytic cells, but not regulated (FDR > 0.05

and IncLevelDifference values -0.05 to 0.05). Human sequences were retrieved from UCSC (hg19, Feb. 2009) using R and the Bioconductor packages, Genomic Ranges, Genomic Features, biomaRt and BSgenome.Hsapiens.UCSC.hg19 (63-65). Graphical outputs were generated with the CRAN package ggplot2. For boxplots, the whiskers represent 1.5 times the interquartile range. Statistical analysis comparing sequences properties between data sets were done using Two sided Mann-Whitney test in R. Sequence logos were produced using WebLogo (http://weblogo.berkeley.edu/logo.cgi) (66). Splice site strength was calculated using MaxEntScan software (http://genes.mit.edu/burgelab/maxent/Xmaxentscan_scoreseq_acc.html) (67). We extracted sequences following developer's instructions for 3SS and 5SS. MaxEnt scores were plotted using ggplot2. Branch point scores and distance between branch point and 3'ss was obtained using SVM-BPfinder (http://regulatorygenomics.upf.edu/Software/SVM_BP/) (68). Data was filtered by restricting the predicted BP to be located between the 3'ss and 12 bp upstream of the agez, and selecting the top svm_scr scoring for each event.

Statistics

The significance of the comparisons between cells transduced with *U2AF1*^{S34F}, *U2AF1*^{WT} or EV was determined by One-Way ANOVA with repeated measures using Tukey's post-tests. The measurements of cell growth over time for cells transduced with *U2AF1*^{S34F}, *U2AF1*^{WT} or EV were compared using two-way ANOVA and Bonferroni post-tests. Comparisons of each type of aberrantly spliced events identified by rMATS between erythroid and granulomocytic conditions were determined by Fisher's exact test with Bonferroni correction. *P* values < 0.05 were considered statistically significant.

Study approval

The MDS patient samples used in this study were obtained with written informed consent under approval by the Institutional Review Boards of the Karolinska Institutet and of the IRCSS Policlinico San Matteo.

Information regarding Real-time quantitative PCR, Western blot, Cell Growth Assay, May-Grünwald-Giemsa staining, Pyrosequencing, SYBR green real-time qPCR, and Cloning and Sanger sequencing can be found in Supplemental Methods.

Author contributions

BHY, VS, RNA, SR, JS, HD, MB conducted experiments. BHY, ER, ML, ST, AV, PV, NCPC, CWJS, AP and JB analyzed data. LM, MC, EHL and SO provided essential samples or reagents for the study. BHY, CWJS, AP and JB designed the study. BHY, ER, ML, CWJS, AP and JB wrote the manuscript.

Acknowledgments

This work was supported by Bloodwise (United Kingdom). ML was supported by a grant from the Wellcome Trust (092900). LM acknowledges support by the Associazione Italiana Ricerca sul Cancro (AIRC, IG 15356). We are grateful to Simon McGowan (Computational Biology Research Group, Weatherall Institute of Molecular Medicine, University of Oxford, Oxford, UK) for advice regarding RNA-seq data analysis.

References

1. Cazzola M, Della Porta MG, Malcovati L. The genetic basis of myelodysplasia and its clinical relevance. *Blood*. 2013;122(25):4021-4034.
2. Greenberg PL, et al. Revised international prognostic scoring system for myelodysplastic syndromes. *Blood*. 2012;120(12):2454-2465.
3. Pellagatti A, Boultwood J. The molecular pathogenesis of the myelodysplastic syndromes. *Eur J Haematol*. 2015;95(1):3-15.
4. Vardiman JW, et al. The 2008 revision of the World Health Organization (WHO) classification of myeloid neoplasms and acute leukemia: rationale and important changes. *Blood*. 2009;114(5):937-951.
5. Papaemmanuil E, et al. Clinical and biological implications of driver mutations in myelodysplastic syndromes. *Blood*. 2013;122(22):3616-3627; quiz 3699.
6. Yoshida K, et al. Frequent pathway mutations of splicing machinery in myelodysplasia. *Nature*. 2011;478(7367):64-69.
7. Papaemmanuil E, et al. Somatic SF3B1 mutation in myelodysplasia with ring sideroblasts. *N Engl J Med*. 2011;365(15):1384-1395.
8. Makishima H, et al. Mutations in the spliceosome machinery, a novel and ubiquitous pathway in leukemogenesis. *Blood*. 2012;119(14):3203-3210.
9. Malcovati L, et al. Clinical significance of SF3B1 mutations in myelodysplastic syndromes and myelodysplastic/myeloproliferative neoplasms. *Blood*. 2011;118(24):6239-6246.
10. Patnaik MM, et al. SF3B1 mutations are prevalent in myelodysplastic syndromes with ring sideroblasts but do not hold independent prognostic value. *Blood*. 2012;119(2):569-572.

11. Damm F, et al. Mutations affecting mRNA splicing define distinct clinical phenotypes and correlate with patient outcome in myelodysplastic syndromes. *Blood*. 2012;119(14):3211-3218.

12. Dolatshad H, et al. Cryptic splicing events in the iron transporter ABCB7 and other key target genes in SF3B1-mutant myelodysplastic syndromes. *Leukemia*. 2016;30(12):2322-2331.

13. Kim E, et al. SRSF2 Mutations Contribute to Myelodysplasia by Mutant-Specific Effects on Exon Recognition. *Cancer Cell*. 2015;27(5):617-630.

14. Pan Q, Shai O, Lee LJ, Frey BJ, Blencowe BJ. Deep surveying of alternative splicing complexity in the human transcriptome by high-throughput sequencing. *Nat Genet*. 2008;40(12):1413-1415.

15. Ruskin B, Zamore PD, Green MR. A factor, U2AF, is required for U2 snRNP binding and splicing complex assembly. *Cell*. 1988;52(2):207-219.

16. Wu S, Romfo CM, Nilsen TW, Green MR. Functional recognition of the 3' splice site AG by the splicing factor U2AF35. *Nature*. 1999;402(6763):832-835.

17. Graubert TA, et al. Recurrent mutations in the U2AF1 splicing factor in myelodysplastic syndromes. *Nat Genet*. 2012;44(1):53-57.

18. Brooks AN, et al. A pan-cancer analysis of transcriptome changes associated with somatic mutations in U2AF1 reveals commonly altered splicing events. *PLoS One*. 2014;9(1):e87361.

19. Yoshida K, Ogawa S. Splicing factor mutations and cancer. *Wiley Interdiscip Rev RNA*. 2014;5(4):445-459.

20. Wu L, et al. Genetic landscape of recurrent ASXL1, U2AF1, SF3B1, SRSF2, and EZH2 mutations in 304 Chinese patients with myelodysplastic syndromes. *Tumour Biol*. 2016;37(4):4633-4640.

21. Wu SJ, et al. Clinical implications of U2AF1 mutation in patients with myelodysplastic syndrome and its stability during disease progression. *Am J Hematol*. 2013;88(11):E277-282.

22. Yoshida H, et al. A novel 3' splice site recognition by the two zinc fingers in the U2AF small subunit. *Genes Dev*. 2015;29(15):1649-1660.

23. Ilagan JO, et al. U2AF1 mutations alter splice site recognition in hematological malignancies. *Genome Res*. 2015;25(1):14-26.

24. Przychodzen B, et al. Patterns of missplicing due to somatic U2AF1 mutations in myeloid neoplasms. *Blood*. 2013;122(6):999-1006.

25. Okeyo-Owuor T, et al. U2AF1 mutations alter sequence specificity of pre-mRNA binding and splicing. *Leukemia*. 2015;29(4):909-917.

26. Shirai CL, et al. Mutant U2AF1 Expression Alters Hematopoiesis and Pre-mRNA Splicing In Vivo. *Cancer Cell*. 2015;27(5):631-643.

27. Caceres G, et al. TP53 suppression promotes erythropoiesis in del(5q) MDS, suggesting a targeted therapeutic strategy in lenalidomide-resistant patients. *Proc Natl Acad Sci U S A*. 2013;110(40):16127-16132.

28. Davies C, et al. Silencing of ASXL1 impairs the granulomonocytic lineage potential of human CD34(+) progenitor cells. *Br J Haematol*. 2013;160(6):842-850.

29. Mazzone A, Ricevuti G. Leukocyte CD11/CD18 integrins: biological and clinical relevance. *Haematologica*. 1995;80(2):161-175.

30. Warren MK, Rose WL, Beall LD, Cone J. CD34+ cell expansion and expression of lineage markers during liquid culture of human progenitor cells. *Stem Cells*. 1995;13(2):167-174.

31. Shen S, et al. rMATS: robust and flexible detection of differential alternative splicing from replicate RNA-Seq data. *Proc Natl Acad Sci U S A*. 2014;111(51):E5593-5601.

891 32. Park SM, et al. U2AF35(S34F) Promotes Transformation by Directing Aberrant
892 ATG7 Pre-mRNA 3' End Formation. *Mol Cell*. 2016;62(4):479-490.
893 33. Santini V. Anemia as the Main Manifestation of Myelodysplastic Syndromes. *Semin*
894 *Hematol*. 2015;52(4):348-356.
895 34. Mian SA, et al. Spliceosome mutations exhibit specific associations with epigenetic
896 modifiers and proto-oncogenes mutated in myelodysplastic syndrome.
897 *Haematologica*. 2013;98(7):1058-1066.
898 35. Matsushima T, et al. Prevalence and clinical characteristics of myelodysplastic
899 syndrome with bone marrow eosinophilia or basophilia. *Blood*. 2003;101(9):3386-
900 3390.
901 36. Wimazal F, et al. Mixed-lineage eosinophil/basophil crisis in MDS: a rare form of
902 progression. *Eur J Clin Invest*. 2008;38(6):447-455.
903 37. Pellagatti A, Boultwood J. Splicing factor gene mutations in the myelodysplastic
904 syndromes: impact on disease phenotype and therapeutic applications. *Adv Biol*
905 *Regul*. 2017;63:59-70.
906 38. Daguenet E, Dujardin G, Valcarcel J. The pathogenicity of splicing defects:
907 mechanistic insights into pre-mRNA processing inform novel therapeutic approaches.
908 *EMBO Rep*. 2015;16(12):1640-1655.
909 39. Kralovicova J, Knut M, Cross NC, Vorechovsky I. Identification of U2AF(35)-
910 dependent exons by RNA-Seq reveals a link between 3' splice-site organization and
911 activity of U2AF-related proteins. *Nucleic Acids Res*. 2015;43(7):3747-3763.
912 40. Hernandez-Munoz I, et al. Stable X chromosome inactivation involves the PRC1
913 Polycomb complex and requires histone MACROH2A1 and the CULLIN3/SPOP
914 ubiquitin E3 ligase. *Proc Natl Acad Sci U S A*. 2005;102(21):7635-7640.

915 41. Boulard M, Storck S, Cong R, Pinto R, Delage H, Bouvet P. Histone variant
916 macroH2A1 deletion in mice causes female-specific steatosis. *Epigenetics Chromatin*.
917 2010;3(1):8.
918 42. Yildirim E, et al. Xist RNA is a potent suppressor of hematologic cancer in mice.
919 *Cell*. 2013;152(4):727-742.
920 43. Pehrson JR, Costanzi C, Dharia C. Developmental and tissue expression patterns of
921 histone macroH2A1 subtypes. *J Cell Biochem*. 1997;65(1):107-113.
922 44. Barrero MJ, Sese B, Marti M, Izpisua Belmonte JC. Macro histone variants are
923 critical for the differentiation of human pluripotent cells. *J Biol Chem*.
924 2013;288(22):16110-16116.
925 45. Sporn JC, et al. Histone macroH2A isoforms predict the risk of lung cancer
926 recurrence. *Oncogene*. 2009;28(38):3423-3428.
927 46. Pimentel H, et al. A dynamic alternative splicing program regulates gene expression
928 during terminal erythropoiesis. *Nucleic Acids Res*. 2014;42(6):4031-4042.
929 47. Grimmler M, Otter S, Peter C, Muller F, Chari A, Fischer U. Unrip, a factor
930 implicated in cap-independent translation, associates with the cytosolic SMN complex
931 and influences its intracellular localization. *Hum Mol Genet*. 2005;14(20):3099-3111.
932 48. Jin L, Datta PK. Oncogenic STRAP functions as a novel negative regulator of E-
933 cadherin and p21(Cip1) by modulating the transcription factor Sp1. *Cell Cycle*.
934 2014;13(24):3909-3920.
935 49. Reiner JE, Datta PK. TGF-beta-dependent and -independent roles of STRAP in
936 cancer. *Front Biosci (Landmark Ed)*. 2011;16:105-115.
937 50. Datta PK, Moses HL. STRAP and Smad7 synergize in the inhibition of transforming
938 growth factor beta signaling. *Mol Cell Biol*. 2000;20(9):3157-3167.

939 51. Zhou L, et al. Reduced SMAD7 leads to overactivation of TGF-beta signaling in
940 MDS that can be reversed by a specific inhibitor of TGF-beta receptor I kinase.
941 *Cancer Res*. 2011;71(3):955-963.
942 52. Kole R, Krainer AR, Altman S. RNA therapeutics: beyond RNA interference and
943 antisense oligonucleotides. *Nat Rev Drug Discov*. 2012;11(2):125-140.
944 53. Havens MA, Hastings ML. Splice-switching antisense oligonucleotides as
945 therapeutic drugs. *Nucleic Acids Res*. 2016;44(14):6549-6563.
946 54. Dobin A, et al. STAR: ultrafast universal RNA-seq aligner. *Bioinformatics*.
947 2013;29(1):15-21.
948 55. DeLuca DS, et al. RNA-SeQC: RNA-seq metrics for quality control and process
949 optimization. *Bioinformatics*. 2012;28(11):1530-1532.
950 56. Li H, et al. The Sequence Alignment/Map format and SAMtools. *Bioinformatics*.
951 2009;25(16):2078-2079.
952 57. Liao Y, Smyth GK, Shi W. featureCounts: an efficient general purpose program for
953 assigning sequence reads to genomic features. *Bioinformatics*. 2014;30(7):923-930.
954 58. Liao Y, Smyth GK, Shi W. The Subread aligner: fast, accurate and scalable read
955 mapping by seed-and-vote. *Nucleic Acids Res*. 2013;41(10):e108.
956 59. Robinson MD, McCarthy DJ, Smyth GK. edgeR: a Bioconductor package for
957 differential expression analysis of digital gene expression data. *Bioinformatics*.
958 2010;26(1):139-140.
959 60. Trapnell C, et al. Transcript assembly and quantification by RNA-Seq reveals
960 unannotated transcripts and isoform switching during cell differentiation. *Nat*
961 *Biotechnol*. 2010;28(5):511-515.
962 61. Katz Y, Wang ET, Airoldi EM, Burge CB. Analysis and design of RNA sequencing
963 experiments for identifying isoform regulation. *Nat Methods*. 2010;7(12):1009-1015.

964 62. Young MD, Wakefield MJ, Smyth GK, Oshlack A. Gene ontology analysis for RNA-
965 seq: accounting for selection bias. *Genome Biol*. 2010;11(2):R14.
966 63. Durinck S, Bullard J, Spellman PT, Dudoit S. GenomeGraphs: integrated genomic
967 data visualization with R. *BMC Bioinformatics*. 2009;10:2.
968 64. Durinck S, et al. BioMart and Bioconductor: a powerful link between biological
969 databases and microarray data analysis. *Bioinformatics*. 2005;21(16):3439-3440.
970 65. Lawrence M, et al. Software for computing and annotating genomic ranges. *PLoS*
971 *Comput Biol*. 2013;9(8):e1003118.
972 66. Crooks GE, Hon G, Chandonia JM, Brenner SE. WebLogo: a sequence logo
973 generator. *Genome Res*. 2004;14(6):1188-1190.
974 67. Yeo G, Burge CB. Maximum entropy modeling of short sequence motifs with
975 applications to RNA splicing signals. *J Comput Biol*. 2004;11(2-3):377-394.
976 68. Carvalho SG, Guerra-Sa R, de CMLH. The impact of sequence length and number of
977 sequences on promoter prediction performance. *BMC Bioinformatics*. 2015;16 Suppl
978 19:S5.

Figure Legends

Figure 1. Expression of U2AF1^{S34F} impairs erythroid differentiation. (A) Western blots showing the expression levels of the U2AF1^{S34F} and U2AF1^{WT} protein in transduced erythroid cells harvested on day 11. An anti-U2AF1 antibody was used to measure total U2AF1 protein while an anti-FLAG antibody was used to measure the exogenous U2AF1^{S34F} or U2AF1^{WT} protein produced by the vector. (B-D) Erythroid differentiation measured using expression of CD71 and CD235a cell surface markers by flow cytometry. (B) Non-erythroid ($CD71^{-}CD235a^{-}$) and (C) intermediate erythroid ($CD71^{+}CD235a^{+}$) cell populations on day 11 of culture, and (D) late erythroid ($CD71^{-}CD235a^{+}$) cell population on day 14 of culture. (E) Representative flow cytometry plots showing impaired erythroid differentiation on day 14 (n=8). (F) Photograph of erythroid cell pellets at day 14 of culture for visual determination of hemoglobinization (n=8). (G) Number of burst-forming unit-erythroid (BFU-E) obtained from hematopoietic $CD34^{+}$ progenitors were transduced with EV, *U2AF1*^{WT} and *U2AF1*^{S34F} after 14 days in methylcellulose (colony-forming cell assays). (H) Representative pictures of BFU-E colonies produced from hematopoietic $CD34^{+}$ progenitors transduced with EV, *U2AF1*^{WT} or *U2AF1*^{S34F} respectively (n=7). The scale bar indicates 100µm. (I) Cell counts on *U2AF1*^{S34F} erythroid cells from day 8 to day 14 of culture compared to EV and *U2AF1*^{WT} controls. (J) Apoptosis measured by Annexin V staining and flow cytometry in erythroblasts harvested on day 11 of culture. Results shown in panels B-D were obtained from 8 independent experiments, panels G and I were obtained from 7 independent experiments and results shown in panel J were obtained from 6 independent experiments. Results are shown as mean ± SEM. P values in panels B, C, D, G and J were calculated by 1-way ANOVA with repeated measures using Tukey's post-test. P values in panel I were calculated by 2-way ANOVA using Bonferroni post-test. *P<0.05, **P<0.01 and ***P<0.001.

Figure 2. Expression of U2AF1^{S34F} skews myeloid differentiation towards granulocytes. (A) Expression levels of the U2AF1^{S34F} and U2AF1^{WT} protein in transduced granulomonocytic cells on day 11. Anti-U2AF1 and anti-FLAG antibodies were used to measure total U2AF1 protein and exogenous U2AF1^{S34F} /U2AF1^{WT} protein produced by the vector respectively. (B) Median fluorescence intensity (MFI) of forward scatter (an indication of cell size) of granulomonocytic cells on day 11 and 14. (C) Percentage of CD11b^{+} cells in granulomonocytic cultures on day 11 and 14. (D) Cell counts on *U2AF1*^{S34F} granulomonocytic cells from day 8 (the day when geneticin selection was complete) to day 14 compared to EV and *U2AF1*^{WT} control. (E) Cell cycle analysis on granulomonocytic cells on day 11. (F) Percentage of CD11b^{+} cells in granulomonocytic cultures on day 20. (G-H) Percentages of (G) CD14^{+}CD15^{-} monocytic cells and (H) CD14^{-}CD15^{+} granulocytic cells in granulomonocytic cultures on day 20. (I) Representative flow cytometry plots on day 20 (n=7). (J) Representative images of May-Grünwald/Giemsa stained granulomonocytic cells on day 20 (n=7). The red arrows indicate eosinophils. The scale bar indicates 25 μm. (K) Quantification of eosinophil as % per 100 cells on day 20. (L) Number of colony-forming unit-granulocyte/macrophage (CFU-GM), colony-forming unit-granulocyte (CFU-G) and colony-forming unit-macrophage (CFU-M) obtained from hematopoietic CD34^{+} progenitors transduced with EV, *U2AF1*^{WT} and *U2AF1*^{S34F} after 14 days in methylcellulose. Results shown in panels (B), (C), (D), (E), (F), (G), (H), (K) and (L) were obtained from 6, 8, 7, 6, 7, 7, 7, 6 and 7 independent experiments respectively. Results are shown as mean ± SEM. P values in panels B, C, E, F, G, H, K and L were calculated by 1-way ANOVA with repeated measures using Tukey's post-test. P values in panel D were calculated by 2-way ANOVA using Bonferroni post-test. *P<0.05, **P<0.01 and ***P<0.001.

Figure 3. *U2AF1*^{S34F} differentially alters splicing of target genes in erythroid and granulomonocytic colonies. (A) Quantification of *U2AF1* wildtype (TCT) and S34F mutant (TTT) mRNA in erythroid and granulomonocytic colonies, determined by pyrosequencing. (B-C) Aberrant splicing events associated with *U2AF1*^{S34F}, including breakdown by event type, in erythroid and granulomonocytic colonies for (B) *U2AF1*^{S34F} versus EV and (C) *U2AF1*^{S34F} versus *U2AF1*^{WT}. A3SS, alternative 3' splice site; A5SS, alternative 5' splice site; MXE, mutually exclusive exons; RI, retained intron; SE, cassette exon. (D) Sequence logos for 3´ splice sites of cassette exons that are unaffected (top row) more included (middle row) or more skipped (bottom row) in response to *U2AF1*^{S34F} compared to *U2AF1*^{WT}. (E) Distribution of exon inclusion and skipping events within the total number of regulated cassette exon events in the comparison of *U2AF1*^{S34F} vs *U2AF1*^{WT} in erythroid and granulomonocytic colonies. (F) Venn diagram showing the overlap among the genes that contain aberrant splicing events induced by *U2AF1*^{S34F} in erythroid colonies and granulomonocytic colonies in our study. (G-J) Venn diagrams showing the overlap among the genes that contain aberrant splicing events induced by *U2AF1*^{S34F} in different RNA-seq datasets: (G) transgenic mouse CMPs expressing U2AF1^{S34F} and erythroid colonies and granulomonocytic colonies in our study, (H) TCGA AML patient samples with *U2AF1* S34 mutations and erythroid colonies and granulomonocytic colonies in our study, (I) *U2AF1*^{S34F} MDS CD34^{+} bone marrow cells (versus MDS cases without splicing factor gene mutations) and erythroid colonies and granulomonocytic colonies in our study, and (J) *U2AF1*^{S34F} MDS CD34^{+} bone marrow cells (versus healthy controls) and erythroid colonies and granulomonocytic colonies in our study. Results in panel A are shown as mean ± SEM and were obtained from 3 independent experiments. P values in panel B and C were calculated by Fisher's exact test with Bonferroni correction. *P<0.05 and **P<0.01.

Figure 4. Confirmation of lineage-specific splicing alterations in *U2AF1*^{S34F} erythroid and granulomonocytic cells. (A) Genes of interest that exhibit differential aberrant splicing between *U2AF1*^{S34F} erythroid and granulomonocytic colonies (*H2AFY* and *STRAP*). (B-C) Mutually exclusive exons in *H2AFY* measured by (B) isoform specific q-RT-PCR and confirmed by (C) RT-PCR and gel electrophoresis. (D-E) Exon skipping in *STRAP* measured by (D) isoform specific q-RT-PCR and confirmed by (E) RT-PCR and gel electrophoresis. In panel (B) and (D), sashimi plots illustrate RNA sequencing results of *H2AFY* and *STRAP* in erythroid and granulomonocytic colonies. For each gene, the region affected by aberrant splicing is shown and the aberrant splicing event is highlighted in grey. In panel (D) the qPCR is specific for the long STRAP isoform, as it was not possible to design a qPCR specific for the short isoform (as there are no unique exons that are specific for the short isoform). The decrease in expression levels of the long STRAP isoform observed in U2AF1^{S34F} erythroid cells is due to the aberrant splicing which removes exon 2 from the long isoform, resulting in the generation of the short isoform and the concomitant depletion of the long isoform. Expression of the isoform associated with aberrant splicing by *U2AF1*^{S34F} in transduced cells was measured by isoform-specific qRT-PCR relative to *U2AF1*^{WT} and EV controls (red bars: erythroid cells; blue bars: granulomonocytic cells). In panel (C) and (E), quantification of altered splicing events in gel was performed by ImageJ. Results in each bar graph were obtained from 5 independent experiments in panels (B-E). Results are shown as mean ± SEM. P values in panels B, C, D and E were calculated by 1-way ANOVA with repeated measures using Tukey's post-test. *P<0.05 and **P<0.01.

Figure 5. Knockdown of *H2AFY* isoform 1.1 perturbs erythroid and granulomonocytic differentiation. (A-B) Expression levels of *H2AFY* (A) isoform 1.1 and (B) isoform 1.2 determined using isoform-specific qRT-PCR in erythroid cells with *H2AFY* isoform 1.1

knockdown. (C) Photograph of erythroid cell pellets at day 14 of culture for visual determination of hemoglobinization (n=6). (D-E) Erythroid differentiation measured using expression of CD71 and CD235a cell surface markers by flow cytometry. (D) Intermediate erythroid ($CD71^+CD235a^+$) cell population on day 11 of culture and (E) late erythroid ($CD71^-CD235a^+$) cell population on day 14 of culture. (F) Number of burst-forming unit-erythroid (BFU-E) obtained from hematopoietic $CD34^+$ progenitors with *H2AFY* isoform 1.1 knockdown after 14 days in methylcellulose (colony-forming cell assays). (G-H) Expression levels of *H2AFY* (G) isoform 1.1 and (H) isoform 1.2 determined using isoform-specific qRT-PCR in granulomonocytic cells with *H2AFY* isoform 1.1 knockdown. (I) Percentage of $CD14^+CD15^+$ cells in granulomonocytic cultures on day 20 of culture. (J) Representative contour plots showing expression of CD14 and CD15 on day 20 of culture by flow cytometry (n=8). (K) Representative images of May-Grünwald/Giemsa stained granulomonocytic cells on day 20 of culture (n=8). The red arrows indicate eosinophils. The scale bar indicates 25 μm. Results in each bar graph were obtained from 6 independent experiments in panel (A), (B), (D), (E), (F), (G) and (H), and 8 independent experiments in panel (I). Results are shown as mean ± SEM. P values in panels A, B, D-I were calculated by 1-way ANOVA with repeated measures using Tukey's post-test. *P<0.05, **P<0.01 and ***P<0.001.

Figure 6. Knockdown of *STRAP* impairs erythroid differentiation and overexpression of *ITGB3BP* is dispensable for granulomonocytic differentiation. (A) Expression levels of *STRAP* determined using qRT-PCR in erythroid cells with *STRAP* knockdown. (B) Cell cycle analysis of erythroid cells on day 11 culture. (C) Photograph of erythroid cell pellets at day 14 of culture for visual determination of hemoglobinization (n=6). (D) Percentage of late erythroid ($CD71^-CD235a^+$) cell population on day 14 of culture. (E) Number of burst-forming unit-erythroid (BFU-E) obtained from hematopoietic $CD34^+$ progenitors with

STRAP knockdown after 14 days in methylcellulose (colony-forming cell assays). (F) Western blots showing the expression levels of the ITGB3BP protein in granulomonocytic cells with *ITGB3BP* overexpression. (G) Cell cycle analysis of granulomonocytic cells on day 11 of culture. (H) Percentage of $CD14^+$ cells in granulomonocytic cultures on day 20 of culture. (I) Percentage of $CD15^+$ cells in granulomonocytic cultures on day 20 of culture. (J) Representative contour plots (from 6 independent experiments) showing expression of CD14 and CD15 on day 20 of culture by flow cytometry. (K) Representative images of May-Grünwald/Giemsa stained granulomonocytic cells on day 20 of culture (n=6). The red arrows indicate eosinophils. The scale bar indicates 25 μm. Results in each bar graph in panel (A), (B), (D), (E), (G), (H) and (I) were obtained from 6 independent experiments. Results are shown as mean ± SEM. P values in panels A, B, D and E were calculated by 1-way ANOVA with repeated measures using Tukey's post-test. P values in panels H and I were calculated by paired 2-tailed t-test.*P<0.05, **P<0.01 and ***P<0.001.

Figure 7. Effects of *H2AFY* isoform 1.1 and *STRAP* long isoform overexpression on erythroid and granulomonocytic differentiation in *U2AF1*^{S34F} MDS patient hematopoietic progenitors. (A) *H2AFY* isoform 1.1 ratio in *U2AF1*^{S34F} MDS differentiated erythroblasts and granulomonocytic cells (day 7 in culture) compared to healthy controls. Arrows indicate *H2AFY* isoform 1.1. (B) *STRAP* short isoform ratio in *U2AF1*^{S34F} MDS differentiated erythroblasts (day 7 in culture) compared to healthy controls. Arrows indicate *STRAP* short isoform. (C-E) Impaired erythropoiesis and skewed differentiation towards granulocytes in *U2AF1*^{S34F} MDS hematopoietic progenitors compared to healthy controls. (C) Late erythroid ($CD71^-CD235a^+$) cell population on day 14 of culture, and (D) monocytic ($CD14^+CD15^-$) and (E) granulocytic ($CD14^-CD15^+$) cell populations on day 20 of culture were measured by flow cytomtery. (F-G) Overexpression of (F) *H2AFY* isoform 1.1 and (G)

STRAP long isoform in *U2AF1*^{S34F} MDS hematopoietic progenitors differentiating towards erythroid and granulomonocytic lineages. Arrows indicate *H2AFY* isoform 1.1 or *STRAP* short isoform. (H-K) Effects of *H2AFY* isoform 1.1 and *STRAP* long isoform overexpression on erythroid and granulomonocytic differentiation of *U2AF1*^{S34F} MDS hematopoietic progenitors. Late erythroid ($CD71^{-}CD235a^{+}$) cell population in transduced erythroblasts expressing *H2AFY* isoform 1.1 (H) or *STRAP* long isoform (I) measured by flow cytometry on day 14 of culture compared to the EV control. (J) Monocytic ($CD14^{+}CD15^{-}$) and (K) granulocytic ($CD14^{-}CD15^{+}$) cell populations in transduced granulomonocytic cells expressing *H2AFY* isoform 1.1 were measured by flow cytomtery on day 20 of culture compared to the EV control. In panel (A-B), quantification of altered splicing events in gel was performed by ImageJ. Results in each bar graph of panels A and B were obtained from 4 technical replicates. Results are shown as mean ± SEM. P values in panels A-E were calculated by unpaired 2-tailed t-test. P values in panels H-K were calculated by paired 2-tailed t-test. *P<0.05, **P<0.01 and ***P<0.001.

Figures

Each figure and its legend are shown on the same page. All figure legends are also available above.

Figure 1

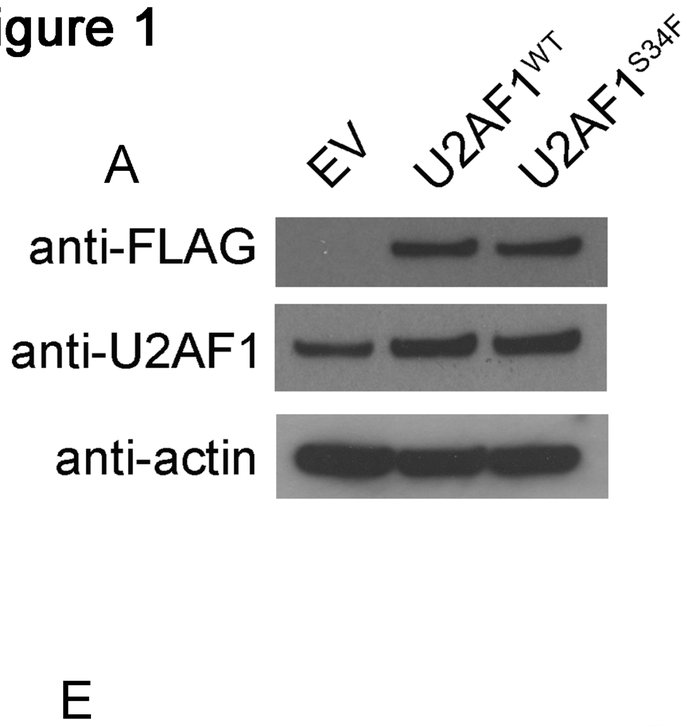

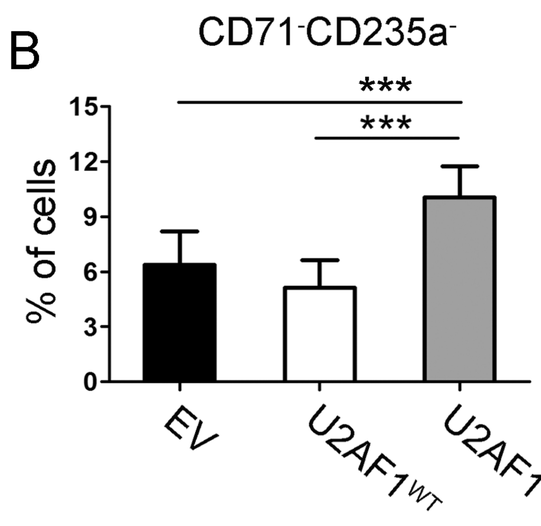

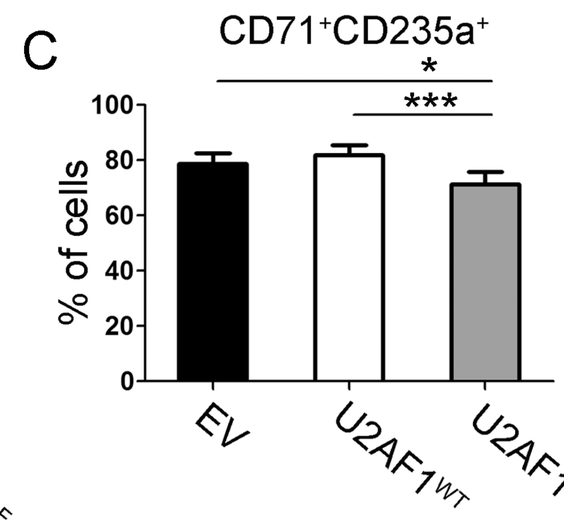

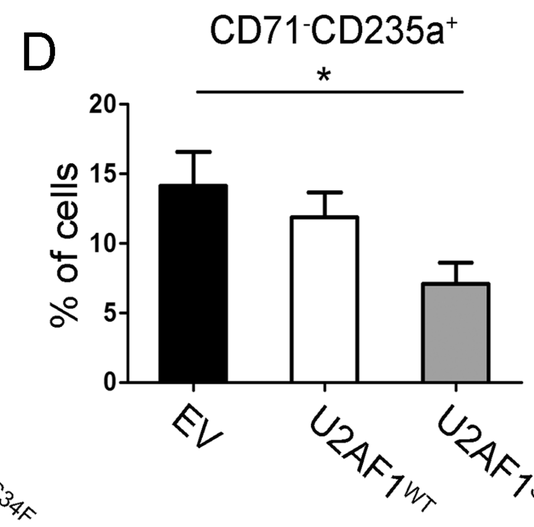

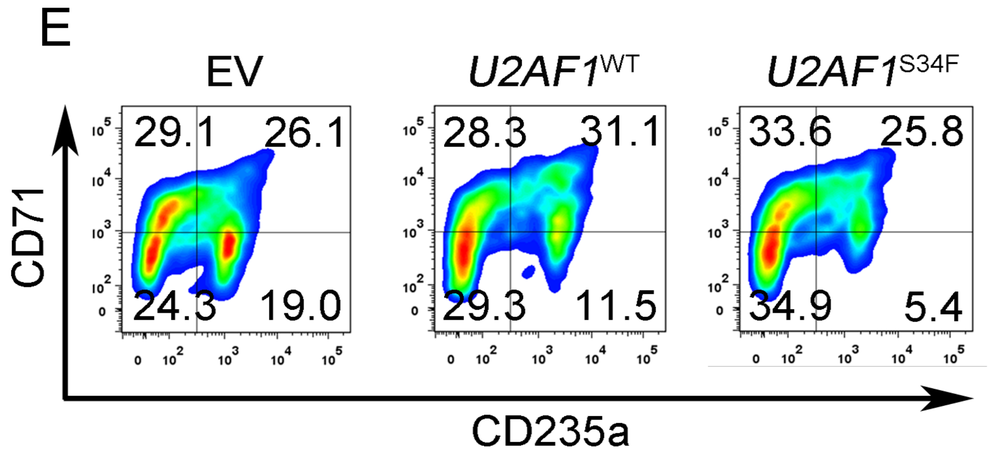

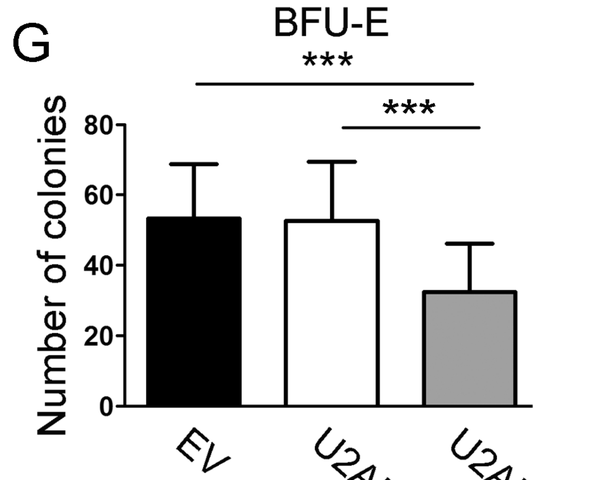

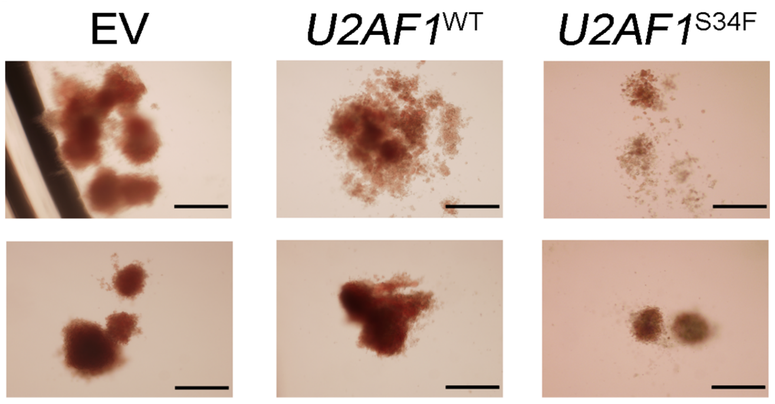

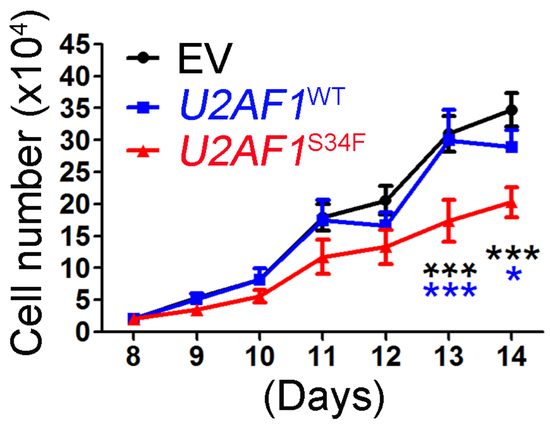

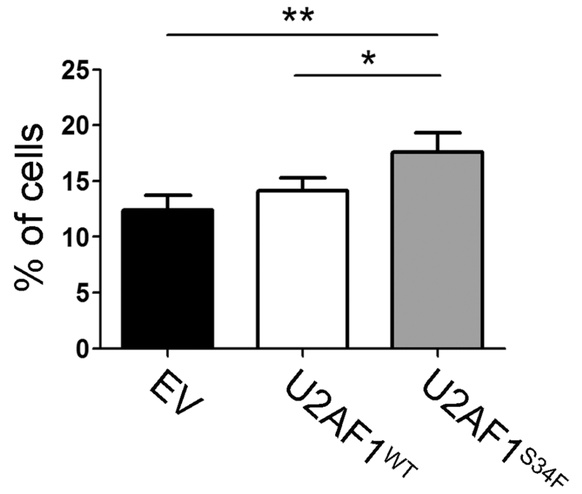

Figure 1. Expression of U2AF1^{S34F} impairs erythroid differentiation. (A) Western blots showing the expression levels of the U2AF1^{S34F} and U2AF1^{WT} protein in transduced erythroid cells harvested on day 11. An anti-U2AF1 antibody was used to measure total U2AF1 protein while an anti-FLAG antibody was used to measure the exogenous U2AF1^{S34F} or U2AF1^{WT} protein produced by the vector. (B-D) Erythroid differentiation measured using expression of CD71 and CD235a cell surface markers by flow cytometry. (B) Non-erythroid (CD71^{-}CD235a^{-}) and (C) intermediate erythroid (CD71^{+}CD235a^{+}) cell populations on day 11 of culture, and (D) late erythroid (CD71^{-}CD235a^{+}) cell population on day 14 of culture. (E) Representative flow cytometry plots showing impaired erythroid differentiation on day 14 (n=8). (F) Photograph of erythroid cell pellets at day 14 of culture for visual determination of hemoglobinization (n=8). (G) Number of burst-forming unit-erythroid (BFU-E) obtained from hematopoietic CD34^{+} progenitors were transduced with EV, *U2AF1*^{WT} and *U2AF1*^{S34F} after 14 days in methylcellulose (colony-forming cell assays). (H) Representative pictures of BFU-E colonies produced from hematopoietic CD34^{+} progenitors transduced with EV, *U2AF1*^{WT} or *U2AF1*^{S34F} respectively (n=7). The scale bar indicates 100µm. (I) Cell counts on *U2AF1*^{S34F} erythroid cells from day 8 to day 14 of culture compared to EV and *U2AF1*^{WT} controls. (J) Apoptosis measured by Annexin V staining and flow cytometry in erythroblasts harvested on day 11 of culture. Results shown in panels B-D were obtained from 8 independent experiments, panels G and I were obtained from 7 independent experiments and results shown in panel J were obtained from 6 independent experiments. Results are shown as mean ± SEM. P values in panels B, C, D, G and J were calculated by 1-way ANOVA with repeated measures using Tukey's post-test. P values in panel I were calculated by 2-way ANOVA using Bonferroni post-test. *P<0.05, **P<0.01 and ***P<0.001.

Figure 2

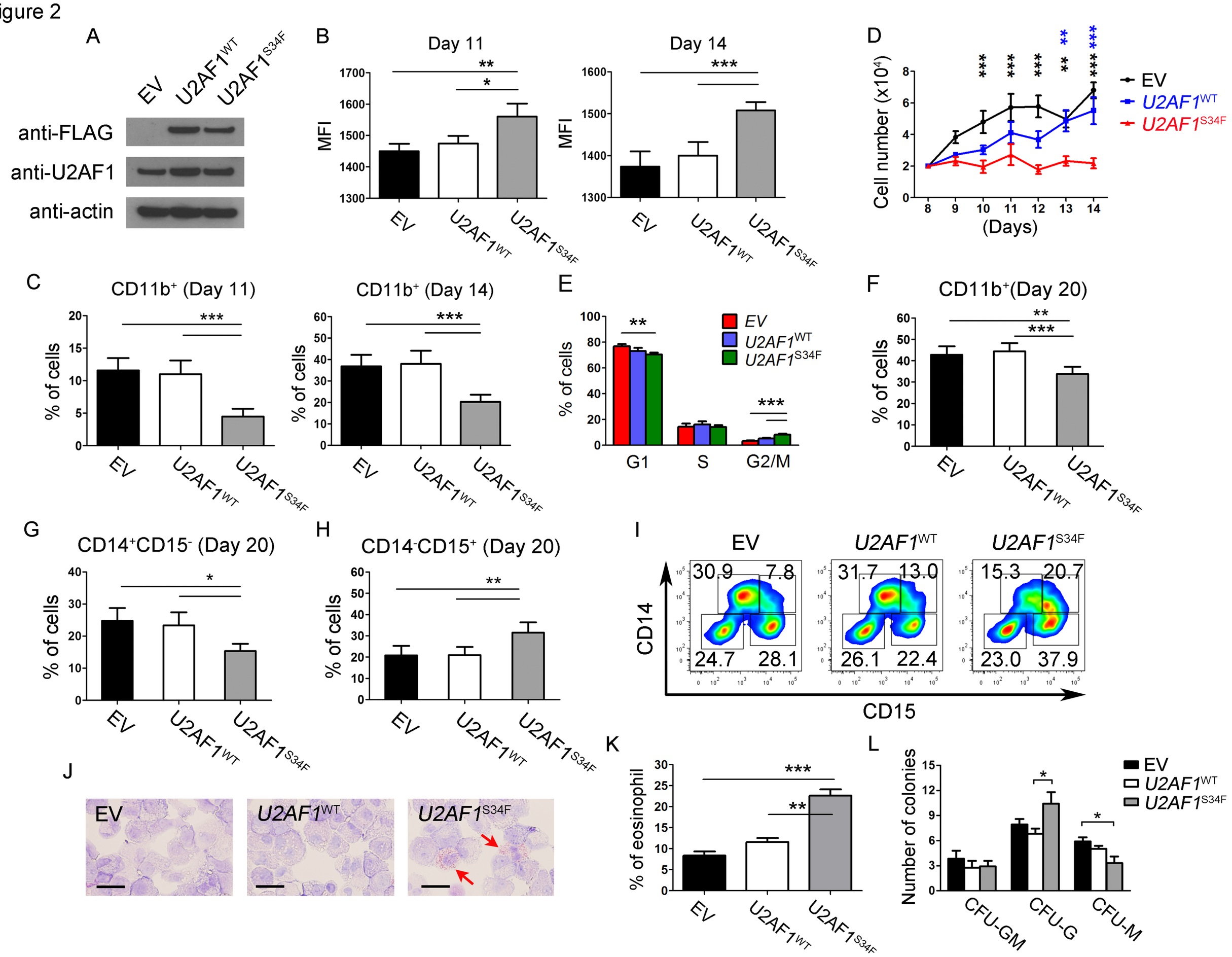

Figure 2. Expression of U2AF1^{S34F} skews myeloid differentiation towards granulocytes. (A) Expression levels of the U2AF1^{S34F} and U2AF1^{WT} protein in transduced granulomonocytic cells on day 11. Anti-U2AF1 and anti-FLAG antibodies were used to measure total U2AF1 protein and exogenous U2AF1^{S34F} /U2AF1^{WT} protein produced by the vector respectively. (B) Median fluorescence intensity (MFI) of forward scatter (an indication of cell size) of granulomonocytic cells on day 11 and 14. (C) Percentage of CD11b^{+} cells in granulomonocytic cultures on day 11 and 14. (D) Cell counts on *U2AF1*^{S34F} granulomonocytic cells from day 8 (the day when geneticin selection was complete) to day 14 compared to EV and *U2AF1*^{WT} control. (E) Cell cycle analysis on granulomonocytic cells on day 11. (F) Percentage of CD11b^{+} cells in granulomonocytic cultures on day 20. (G-H) Percentages of (G) CD14^{+}CD15^{-} monocytic cells and (H) CD14^{-}CD15^{+} granulocytic cells in granulomonocytic cultures on day 20. (I) Representative flow cytometry plots on day 20 (n=7). (J) Representative images of May-Grünwald/Giemsa stained granulomonocytic cells on day 20 (n=7). The red arrows indicate eosinophils. The scale bar indicates 25 μm. (K) Quantification of eosinophil as % per 100 cells on day 20. (L) Number of colony-forming unit-granulocyte/macrophage (CFU-GM), colony-forming unit-granulocyte (CFU-G) and colony-forming unit-macrophage (CFU-M) obtained from hematopoietic CD34^{+} progenitors transduced with EV, *U2AF1*^{WT} and *U2AF1*^{S34F} after 14 days in methylcellulose. Results shown in panels (B), (C), (D), (E), (F), (G), (H), (K) and (L) were obtained from 6, 8, 7, 6, 7, 7, 7, 6 and 7 independent experiments respectively. Results are shown as mean ± SEM. P values in panels B, C, E, F, G, H, K and L were calculated by 1-way ANOVA with repeated measures using Tukey's post-test. P values in panel D were calculated by 2-way ANOVA using Bonferroni post-test. *P<0.05, **P<0.01 and ***P<0.001.

Figure 3

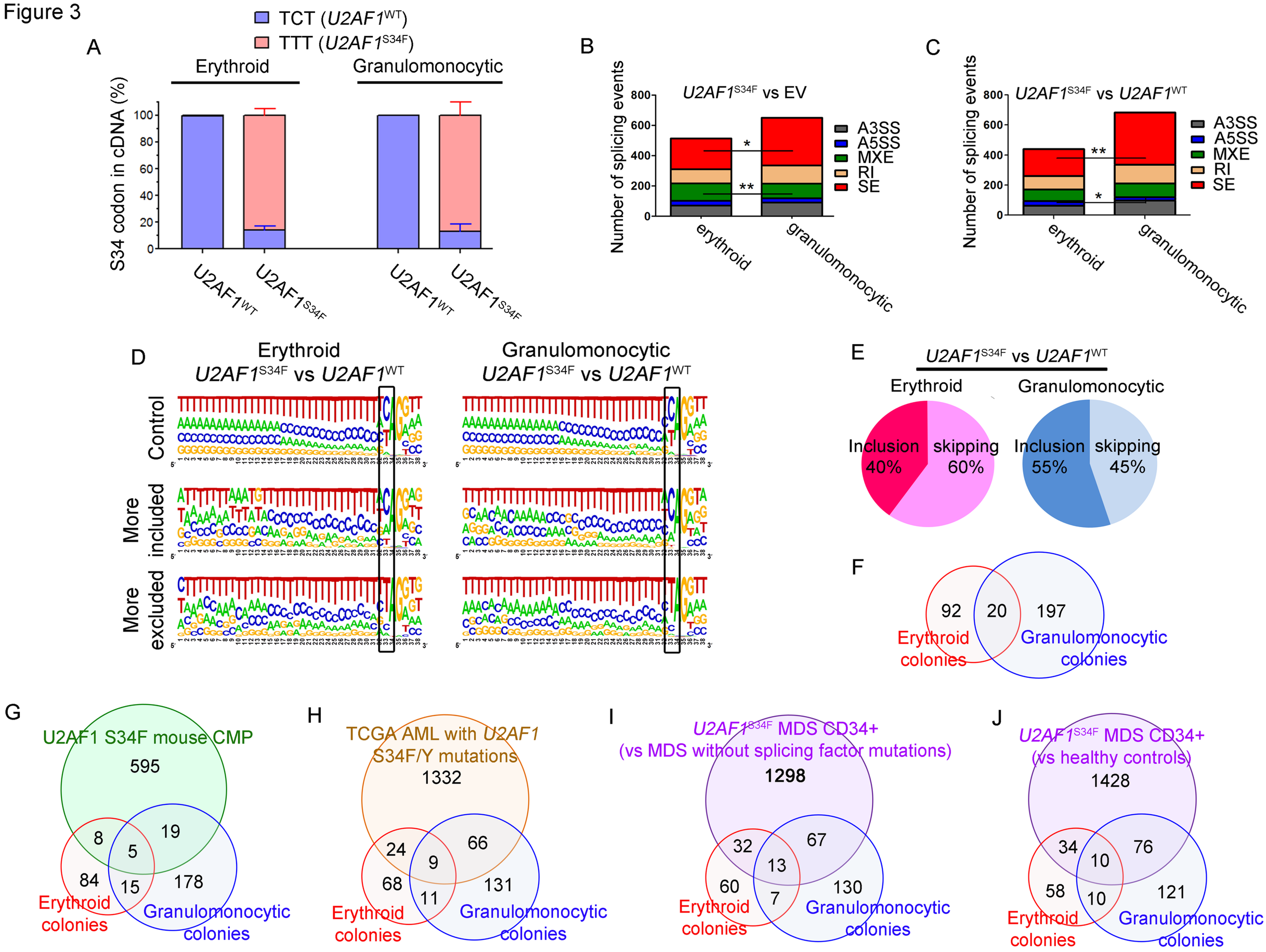

Figure 3. *U2AF1*^{S34F} differentially alters splicing of target genes in erythroid and granulomonocytic colonies. (A) Quantification of *U2AF1* wildtype (TCT) and S34F mutant (TTT) mRNA in erythroid and granulomonocytic colonies, determined by pyrosequencing. (B-C) Aberrant splicing events associated with *U2AF1*^{S34F}, including breakdown by event type, in erythroid and granulomonocytic colonies for (B) *U2AF1*^{S34F} versus EV and (C) *U2AF1*^{S34F} versus *U2AF1*^{WT}. A3SS, alternative 3' splice site; A5SS, alternative 5' splice site; MXE, mutually exclusive exons; RI, retained intron; SE, cassette exon. (D) Sequence logos for 3′ splice sites of cassette exons that are unaffected (top row) more included (middle row) or more skipped (bottom row) in response to *U2AF1*^{S34F} compared to *U2AF1*^{WT}. (E) Distribution of exon inclusion and skipping events within the total number of regulated cassette exon events in the comparison of *U2AF1*^{S34F} vs *U2AF1*^{WT} in erythroid and granulomonocytic colonies. (F) Venn diagram showing the overlap among the genes that contain aberrant splicing events induced by *U2AF1*^{S34F} in erythroid colonies and granulomonocytic colonies in our study. (G-J) Venn diagrams showing the overlap among the genes that contain aberrant splicing events induced by *U2AF1*^{S34F} in different RNA-seq datasets: (G) transgenic mouse CMPs expressing U2AF1^{S34F} and erythroid colonies and granulomonocytic colonies in our study, (H) TCGA AML patient samples with *U2AF1* S34 mutations and erythroid colonies and granulomonocytic colonies in our study, (I) *U2AF1*^{S34F} MDS CD34^{+} bone marrow cells (versus MDS cases without splicing factor gene mutations) and erythroid colonies and granulomonocytic colonies in our study, and (J) *U2AF1*^{S34F} MDS CD34^{+} bone marrow cells (versus healthy controls) and erythroid colonies and granulomonocytic colonies in our study. Results in panel A are shown as mean ± SEM and were obtained from 3 independent experiments. P values in panel B and C were calculated by Fisher's exact test with Bonferroni correction. *P<0.05 and **P<0.01.

Figure 4

A

Gene	Aberrant splicing event	Affected lineage
H2AFY	Reduction in mutually exclusive exon 6b usage	erythroid and granulomonocytic
STRAP	Skipping of exon 2	erythroid

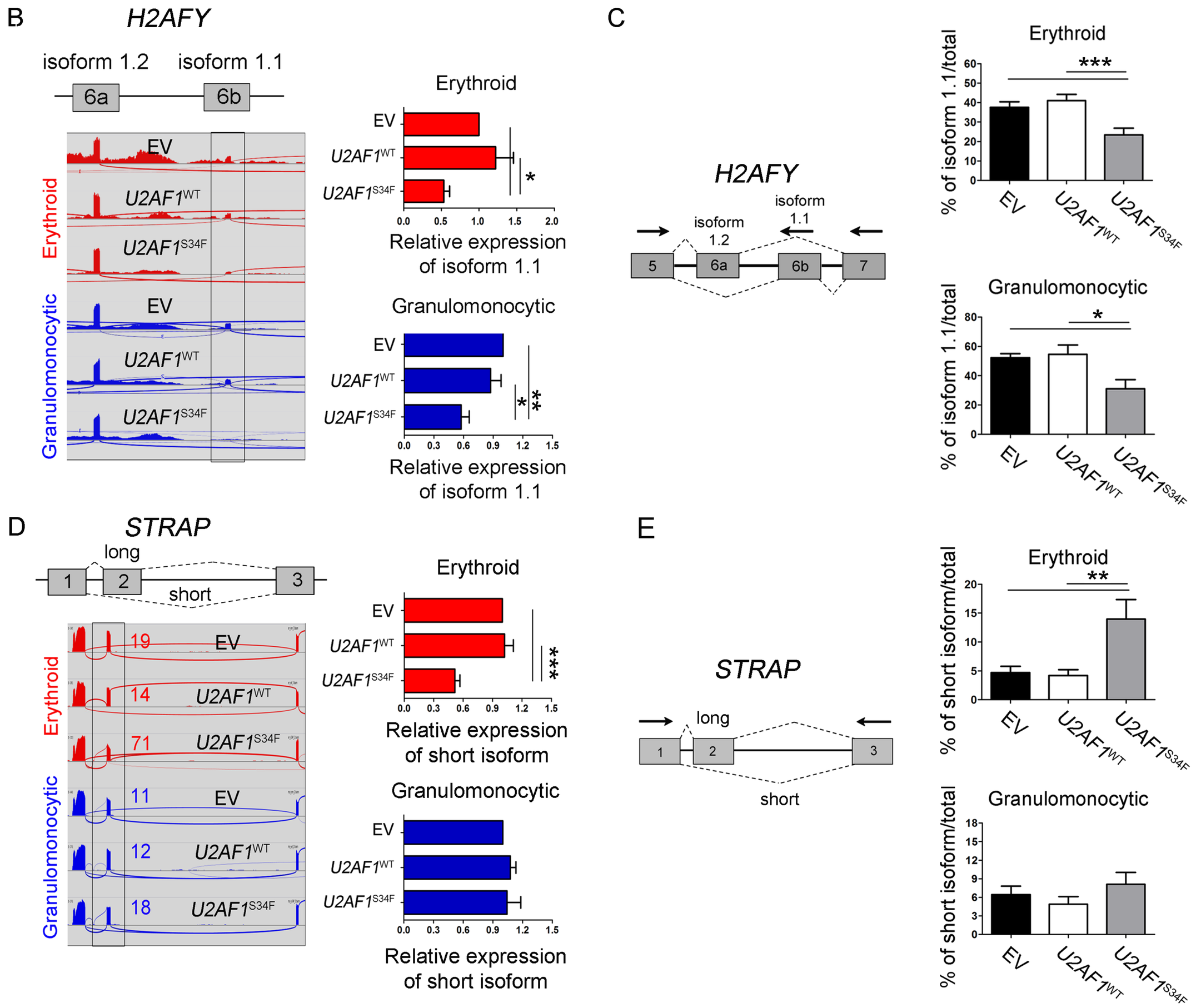

Figure 4. Confirmation of lineage-specific splicing alterations in *U2AF1*^{S34F} erythroid and granulomonocytic cells. (A) Genes of interest that exhibit differential aberrant splicing between *U2AF1*^{S34F} erythroid and granulomonocytic colonies (*H2AFY* and *STRAP*). (B-C) Mutually exclusive exons in *H2AFY* measured by (B) isoform specific q-RT-PCR and confirmed by (C) RT-PCR and gel electrophoresis. (D-E) Exon skipping in *STRAP* measured by (D) isoform specific q-RT-PCR and confirmed by (E) RT-PCR and gel electrophoresis. In panel (B) and (D), sashimi plots illustrate RNA sequencing results of *H2AFY* and *STRAP* in erythroid and granulomonocytic colonies. For each gene, the region affected by aberrant splicing is shown and the aberrant splicing event is highlighted in grey. In panel (D) the qPCR is specific for the long STRAP isoform, as it was not possible to design a qPCR specific for the short isoform (as there are no unique exons that are specific for the short isoform). The decrease in expression levels of the long STRAP isoform observed in U2AF1^{S34F} erythroid cells is due to the aberrant splicing which removes exon 2 from the long isoform, resulting in the generation of the short isoform and the concomitant depletion of the long isoform. Expression of the isoform associated with aberrant splicing by *U2AF1*^{S34F} in transduced cells was measured by isoform-specific qRT-PCR relative to *U2AF1*^{WT} and EV controls (red bars: erythroid cells; blue bars: granulomonocytic cells). In panel (C) and (E), quantification of altered splicing events in gel was performed by ImageJ. Results in each bar graph were obtained from 5 independent experiments in panels (B-E). Results are shown as mean ± SEM. P values in panels B, C, D and E were calculated by 1-way ANOVA with repeated measures using Tukey's post-test. *P<0.05 and **P<0.01.

Figure 5

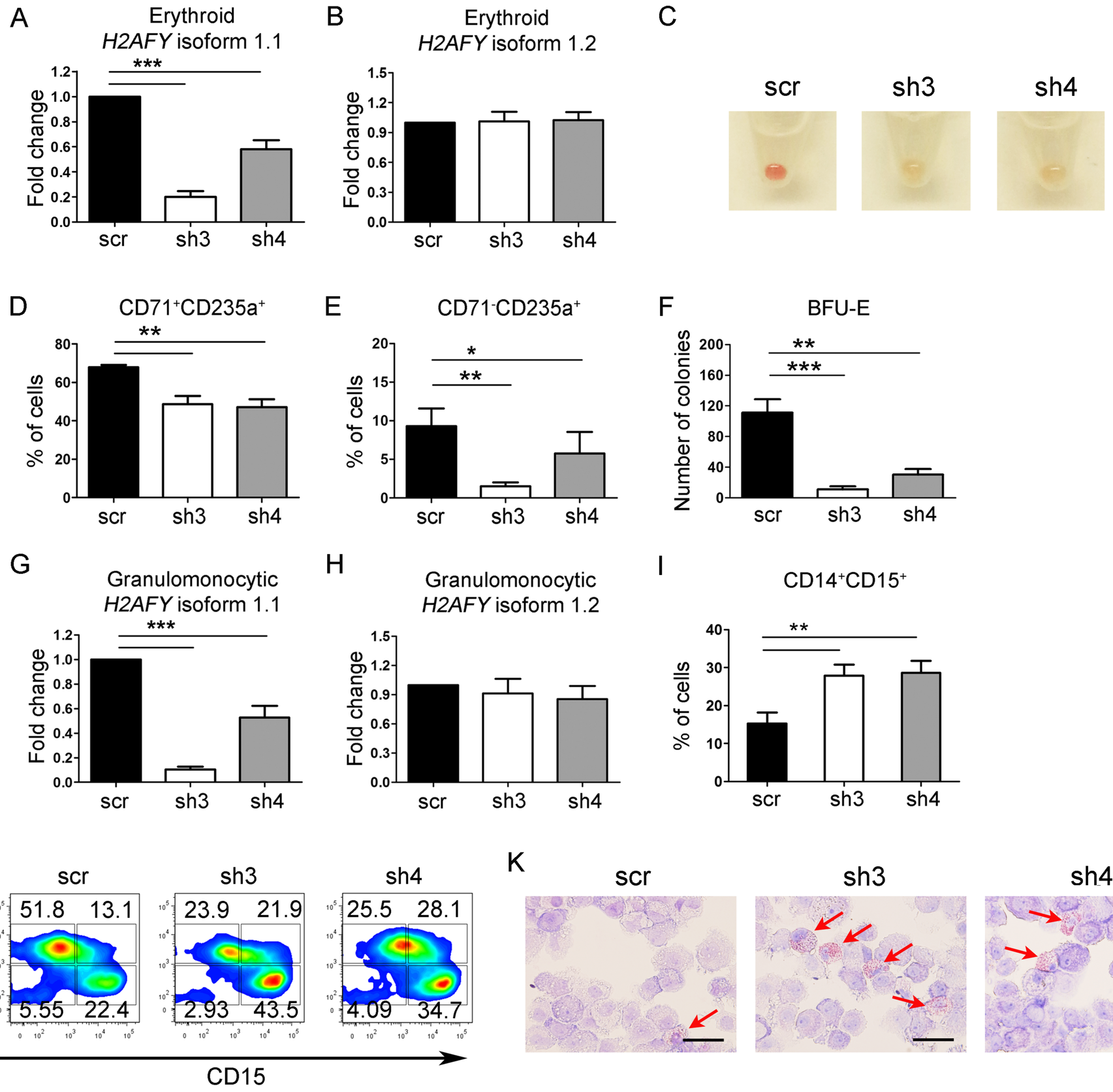

Figure 5. Knockdown of *H2AFY* isoform 1.1 perturbs erythroid and granulomonocytic differentiation. (A-B) Expression levels of *H2AFY* (A) isoform 1.1 and (B) isoform 1.2 determined using isoform-specific qRT-PCR in erythroid cells with *H2AFY* isoform 1.1 knockdown. (C) Photograph of erythroid cell pellets at day 14 of culture for visual determination of hemoglobinization (n=6). (D-E) Erythroid differentiation measured using expression of CD71 and CD235a cell surface markers by flow cytometry. (D) Intermediate erythroid ($CD71^+CD235a^+$) cell population on day 11 of culture and (E) late erythroid ($CD71^-CD235a^+$) cell population on day 14 of culture. (F) Number of burst-forming unit-erythroid (BFU-E) obtained from hematopoietic $CD34^+$ progenitors with *H2AFY* isoform 1.1 knockdown after 14 days in methylcellulose (colony-forming cell assays). (G-H) Expression levels of *H2AFY* (G) isoform 1.1 and (H) isoform 1.2 determined using isoform-specific qRT-PCR in granulomonocytic cells with *H2AFY* isoform 1.1 knockdown. (I) Percentage of $CD14^+CD15^+$ cells in granulomonocytic cultures on day 20 of culture. (J) Representative contour plots showing expression of CD14 and CD15 on day 20 of culture by flow cytometry (n=8). (K) Representative images of May-Grünwald/Giemsa stained granulomonocytic cells on day 20 of culture (n=8). The red arrows indicate eosinophils. The scale bar indicates 25 μm. Results in each bar graph were obtained from 6 independent experiments in panel (A), (B), (D), (E), (F), (G) and (H), and 8 independent experiments in panel (I). Results are shown as mean ± SEM. P values in panels A, B, D-I were calculated by 1-way ANOVA with repeated measures using Tukey's post-test. *P<0.05, **P<0.01 and ***P<0.001.

Figure 6

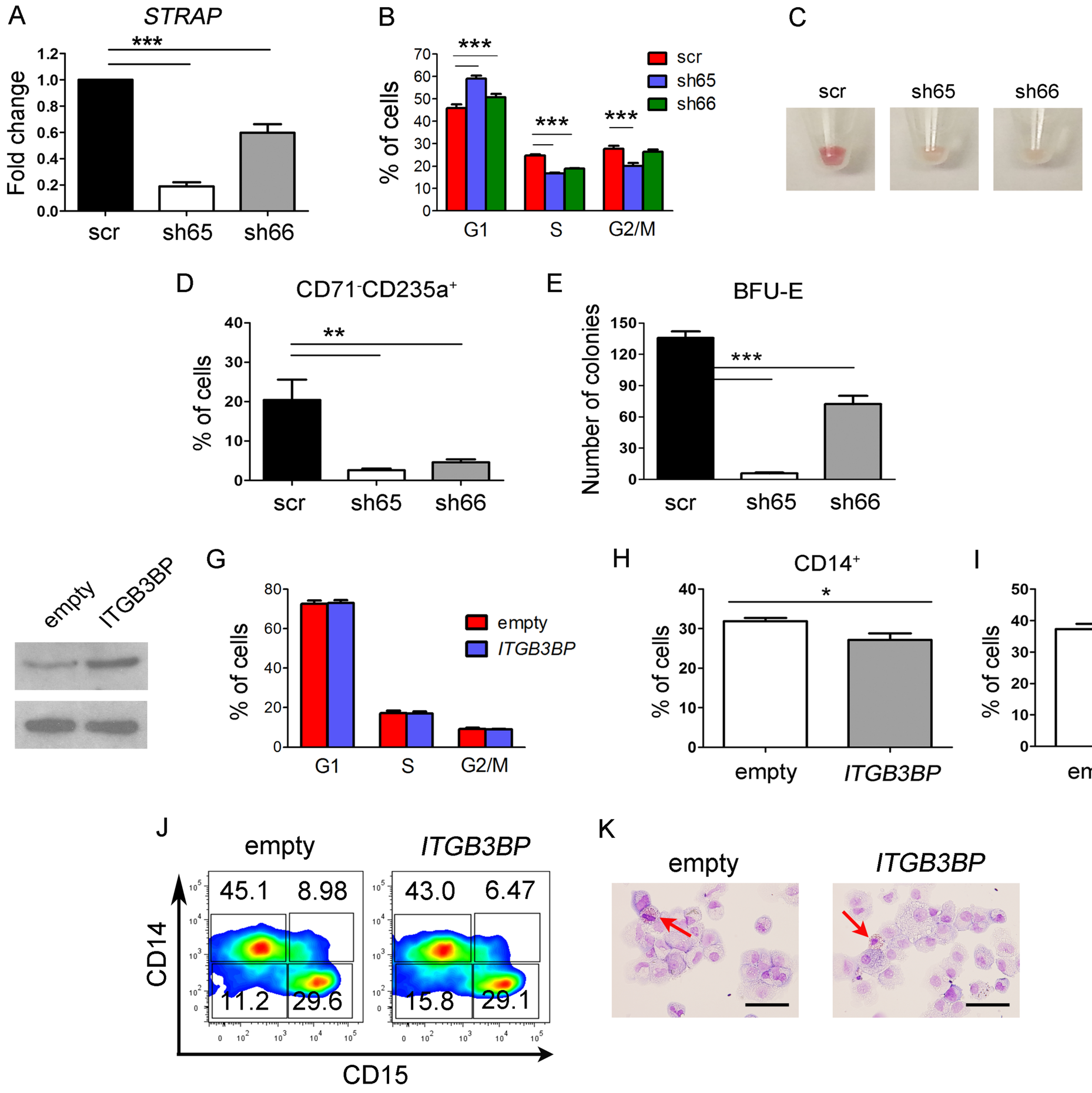

Figure 6. Knockdown of *STRAP* impairs erythroid differentiation and overexpression of *ITGB3BP* is dispensable for granulomonocytic differentiation. (A) Expression levels of *STRAP* determined using qRT-PCR in erythroid cells with *STRAP* knockdown. (B) Cell cycle analysis of erythroid cells on day 11 culture. (C) Photograph of erythroid cell pellets at day 14 of culture for visual determination of hemoglobinization (n=6). (D) Percentage of late erythroid ($CD71^{-}CD235a^{+}$) cell population on day 14 of culture. (E) Number of burst-forming unit-erythroid (BFU-E) obtained from hematopoietic $CD34^{+}$ progenitors with *STRAP* knockdown after 14 days in methylcellulose (colony-forming cell assays). (F) Western blots showing the expression levels of the ITGB3BP protein in granulomonocytic cells with *ITGB3BP* overexpression. (G) Cell cycle analysis of granulomonocytic cells on day 11 of culture. (H) Percentage of $CD14^{+}$ cells in granulomonocytic cultures on day 20 of culture. (I) Percentage of $CD15^{+}$ cells in granulomonocytic cultures on day 20 of culture. (J) Representative contour plots (from 6 independent experiments) showing expression of CD14 and CD15 on day 20 of culture by flow cytometry. (K) Representative images of May-Grünwald/Giemsa stained granulomonocytic cells on day 20 of culture (n=6). The red arrows indicate eosinophils. The scale bar indicates 25 μm. Results in each bar graph in panel (A), (B), (D), (E), (G), (H) and (I) were obtained from 6 independent experiments. Results are shown as mean ± SEM. P values in panels A, D and E were calculated by 1-way ANOVA with repeated measures using Tukey's post-test. P values in panel B were calculated by 2-way ANOVA with repeated measures using Bonferroni post-test. P values in panels H and I were calculated by paired 2-tailed t-test.*P<0.05, **P<0.01 and ***P<0.001.

Figure 7

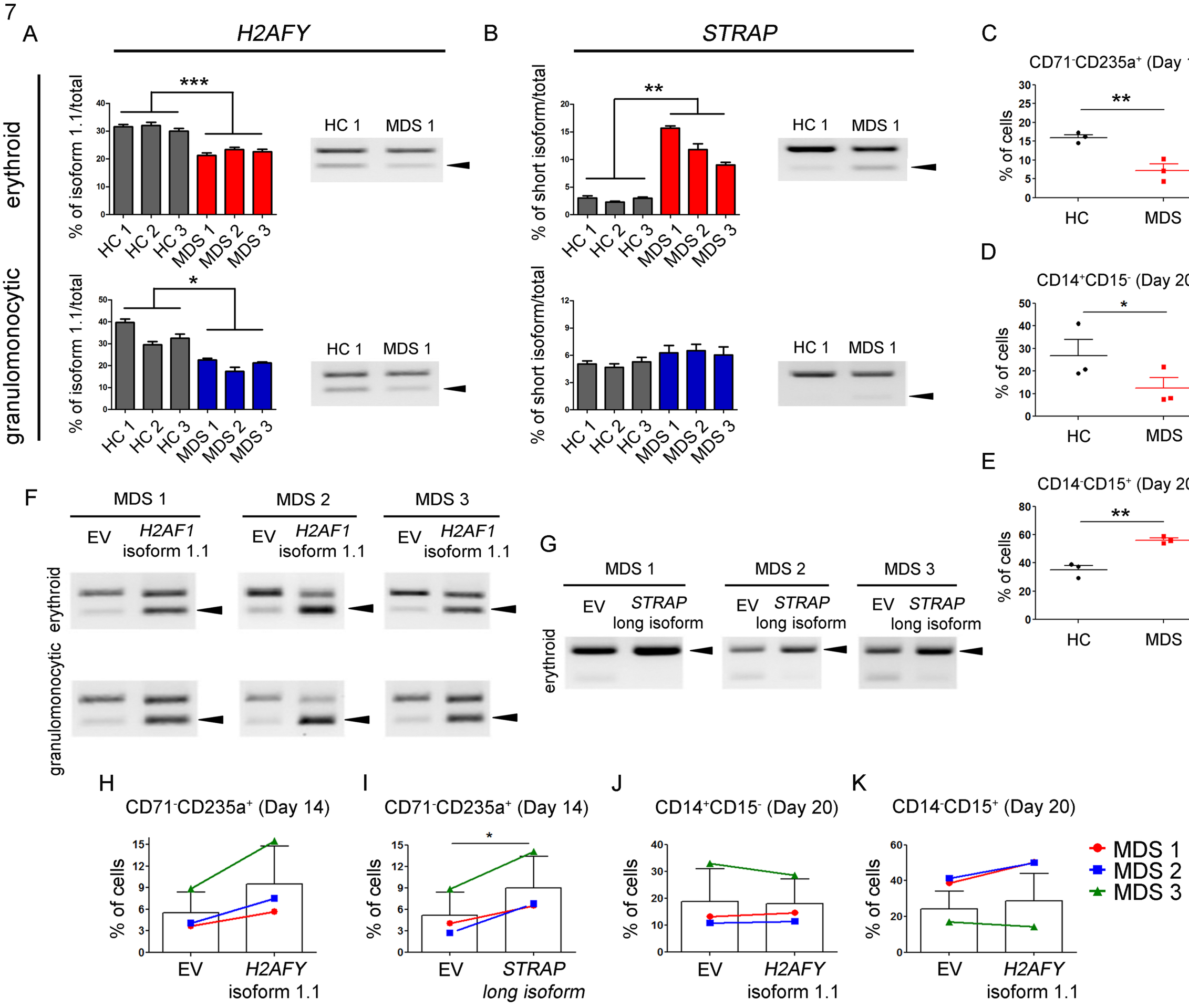

Figure 7. Effects of *H2AFY* isoform 1.1 and *STRAP* long isoform overexpression on erythroid and granulomonocytic differentiation in *U2AF1*^{S34F} MDS patient hematopoietic progenitors. (A) *H2AFY* isoform 1.1 ratio in *U2AF1*^{S34F} MDS differentiated erythroblasts and granulomonocytic cells (day 7 in culture) compared to healthy controls. Arrows indicate *H2AFY* isoform 1.1. (B) *STRAP* short isoform ratio in *U2AF1*^{S34F} MDS differentiated erythroblasts (day 7 in culture) compared to healthy controls. Arrows indicate *STRAP* short isoform. (C-E) Impaired erythropoiesis and skewed differentiation towards granulocytes in *U2AF1*^{S34F} MDS hematopoietic progenitors compared to healthy controls. (C) Late erythroid (CD71^{-}CD235a^{+}) cell population on day 14 of culture, and (D) monocytic (CD14^{+}CD15^{-}) and (E) granulocytic (CD14^{-}CD15^{+}) cell populations on day 20 of culture were measured by flow cytomtery. (F-G) Overexpression of (F) *H2AFY* isoform 1.1 and (G) *STRAP* long isoform in *U2AF1*^{S34F} MDS hematopoietic progenitors differentiating towards erythroid and granulomonocytic lineages. Arrows indicate *H2AFY* isoform 1.1 or *STRAP* short isoform. (H-K) Effects of *H2AFY* isoform 1.1 and *STRAP* long isoform overexpression on erythroid and granulomonocytic differentiation of *U2AF1*^{S34F} MDS hematopoietic progenitors. Late erythroid (CD71^{-}CD235a^{+}) cell population in transduced erythroblasts expressing *H2AFY* isoform 1.1 (H) or *STRAP* long isoform (I) measured by flow cytometry on day 14 of culture compared to the EV control. (J) Monocytic (CD14^{+}CD15^{-}) and (K) granulocytic (CD14^{-}CD15^{+}) cell populations in transduced granulomonocytic cells expressing *H2AFY* isoform 1.1 were measured by flow cytomtery on day 20 of culture compared to the EV control. In panel (A-B), quantification of altered splicing events in gel was performed by ImageJ. Results in each bar graph of panels A and B were obtained from 4 technical replicates. Results are shown as mean ± SEM. P values in panels A-E were calculated by unpaired 2-tailed t-test. P values in panels H-K were calculated by paired 2-tailed t-test. *P<0.05, **P<0.01 and ***P<0.001.